Mapping targets for small nucleolar RNAs in yeast

RESEARCH ARTICLE

REVISED Mapping targets for small nucleolar RNAs in yeast [version 2; peer review: 5 approved]

Tatiana Dudnakova, Hywel Dunn-Davies, Rosie Peters, David Tollervey

Wellcome Centre for Cell Biology, University of Edinburgh, Edinburgh, EH9 3BF, UK

v2 **First published:** 19 Sep 2018, **3**:120 (https://doi.org/10.12688/wellcomeopenres.14735.1)

Latest published: 22 Nov 2018, **3**:120 (https://doi.org/10.12688/wellcomeopenres.14735.2)

Abstract

Background: Recent analyses implicate changes in the expression of the box C/D class of small nucleolar RNAs (snoRNAs) in several human diseases.

Methods: Here we report the identification of potential novel RNA targets for box C/D snoRNAs in budding yeast, using the approach of UV crosslinking and sequencing of hybrids (CLASH) with the snoRNP proteins Nop1, Nop56 and Nop58. We also developed a bioinformatics approach to filter snoRNA-target interactions for bona fide methylation guide interactions.

Results: We recovered 241,420 hybrids, out of which 190,597 were classed as reproducible, high energy hybrids. As expected, the majority of snoRNA interactions were with the ribosomal RNAs (rRNAs). Following filtering, 117,047 reproducible hybrids included 51 of the 55 reported rRNA methylation sites. The majority of interactions at methylation sites were predicted to guide methylation. However, competing, potentially regulatory, binding was also identified. In marked contrast, following CLASH performed with the RNA helicase Mtr4 only 7% of snoRNA-rRNA interactions recovered were predicted to guide methylation. We propose that Mtr4 functions in dissociating inappropriate snoRNA-target interactions. Numerous snoRNA-snoRNA interactions were recovered, indicating potential cross regulation. The snoRNAs snR4 and snR45 were recently implicated in site-directed rRNA acetylation, and hybrids were identified adjacent to the acetylation sites. We also identified 1,368 reproducible snoRNA-mRNA interactions, representing 448 sites of interaction involving 39 snoRNAs and 382 mRNAs. Depletion of the snoRNAs U3, U14 or snR4 each altered the levels of numerous mRNAs. Targets identified by CLASH were over-represented among these species, but causality has yet to be established.

Conclusions: Systematic mapping of snoRNA-target binding provides a catalogue of high-confidence binding sites and indicates numerous potential regulatory interactions.

Keywords

small nucleolar RNA, snoRNA, RNA-RNA interaction, RNA-protein interaction, UV cross-linking

Open Peer Review

Reviewer Status ✓ ✓ ✓ ✓ ✓

	Invited Reviewers				
	1	**2**	**3**	**4**	**5**
REVISED **version 2** published 22 Nov 2018		✓			
version 1 published 19 Sep 2018	✓ report	✓ report	✓ report	✓ report	✓ report

1 **Bruno Charpentier**, University of Lorraine, Nancy, France
Mathieu Rederstorff, University of Lorraine, Nancy, France

2 **Lars Wieslander**, Stockholm University, Stockholm, Sweden

3 **Carla Columbano Oliveira**, University of Sao Paulo, São Paulo, Brazil

4 **Joshua Black**, University of Texas at Austin, Austin, USA
Arlen W. Johnson, University of Texas at Austin, Austin, USA

5 **Pascale Romby**, University of Strasbourg, Strasbourg, France

Any reports and responses or comments on the article can be found at the end of the article.

Corresponding author: David Tollervey (D.Tollervey@ed.ac.uk)

Author roles: Dudnakova T: Formal Analysis, Investigation, Methodology, Visualization, Writing – Original Draft Preparation, Writing – Review & Editing; **Dunn-Davies H**: Data Curation, Formal Analysis, Methodology, Software, Writing – Original Draft Preparation, Writing – Review & Editing; **Peters R**: Investigation, Writing – Original Draft Preparation, Writing – Review & Editing; **Tollervey D**: Conceptualization, Funding Acquisition, Project Administration, Supervision, Visualization, Writing – Original Draft Preparation, Writing – Review & Editing

Competing interests: No competing interests were disclosed.

Grant information: This work was supported by Wellcome Trust Fellowships to D.T. [077248] and R.P. [102311]. T.D and H.D.-D. were supported by BBSRC funding [Bb/L020416/1]. Work in the Wellcome Trust Centre for Cell Biology is supported by Wellcome Trust core funding [092076].
The funders had no role in study design, data collection and analysis, decision to publish, or preparation of the manuscript.

How to cite this article: Dudnakova T, Dunn-Davies H, Peters R and Tollervey D. **Mapping targets for small nucleolar RNAs in yeast [version 2; peer review: 5 approved]** Wellcome Open Research 2018, **3**:120 (https://doi.org/10.12688/wellcomeopenres.14735.2)

First published: 19 Sep 2018, **3**:120 (https://doi.org/10.12688/wellcomeopenres.14735.1)

REVISED **Amendments from Version 1**

The text has been altered in many locations in response to the comments of the referees. Additional discussion and revised versions of Figure 4 and Figure 5 are now included. In response to community feedback, we have included two additional supplementary tables with the filtered list of snoRNA-mRNA interactions (Supplementary Table 3) and the total list of interactions and sites (Supplementary Table 4).

See referee reports

Introduction

The small nucleolar RNAs (snoRNAs) are an abundant class of stable RNAs, most of which act as guides for site-specific RNA modification. Most members of the box C/D class of snoRNAs select sites of ribose 2'-*O*-methylation via extended regions of perfect complementarity with target sites (≥12 bp), in which the nucleotide to be modified is placed exactly 5 bp from the conserved box D or box D' motifs within the snoRNA (reviewed in (Tollervey & Kiss, 1997; Watkins & Bohnsack, 2012)). The box C/D snoRNAs associate with a group of four common proteins, Nop56, Nop58, Snu13 and the methyltransferase Nop1 (Fibrillarin in humans). The snoRNAs have a partially symmetrical structure, in which stem structures bring together the highly conserved, terminal box C (RUGAUGA, R = A or G) and box D (CUGA) sequences and the related but less conserved, internal box C' and box D' elements. These stem structures include a K-turn structural motif that is bound by the small protein Snu13. *In vitro* structural analysis indicated that the box C/D stem is also bound by Nop58, while the box C'/D' stem is bound by the homologous Nop56 protein. Each region is bound by a copy of Nop1, so the regions flanking either box D, box D' or both can function as methylation guides. However, guide function has a strict requirement for a long region of perfect between the snoRNA and the target RNA, which extends to box D or D'. This implies that strong snoRNA base pairing could occur without eliciting target RNA methylation. Indeed, a small number of box C/D snoRNAs have essential functions in ribosome synthesis that require snoRNA/pre-rRNA base pairing without associated RNA methylation. These snoRNAs include U3/snR17 and U14/snR128 in yeast and U3, U14 and U8 in vertebrates (reviewed by Watkins & Bohnsack (2012)). In yeast, all known sites of snoRNA-directed methylation are in the 18S and 25S rRNAs, whereas human snoRNAs can additionally direct methylation of other small RNAs, including spliceosomal small nuclear RNAs (snRNAs) and other snoRNAs.

In yeast, the complete set of rRNA modifications have likely been identified (Taoka *et al.*, 2016; Yang *et al.*, 2016). Bioinformatics approaches have been used to predict snoRNA binding sites in several systems, particularly where this is associated with methylation (Jorjani *et al.*, 2016; Lowe & Eddy, 1999; Lu *et al.*, 2016; Omer *et al.*, 2000). For a listing of yeast snoRNA-target interactions see (https://www-snorna.biotoul.fr/) (Lestrade & Weber, 2006). In addition, a number of recent reports have described methods for the identification of RNA-RNA interactions through proximity ligation followed by sequencing of the products of reverse transcription and PCR amplification (RT-PCR) (Gumienny *et al.*, 2017; Kudla *et al.*, 2011; Sharma *et al.*, 2016; Sugimoto *et al.*, 2015). In the crosslinking and sequencing of hybrids (CLASH) approach, stringent tandem affinity purification including denaturing conditions is used to recover only covalent RNA-protein interactions (Kudla *et al.*, 2011). Here we report the application of CLASH to the identification of novel snoRNA-target interactions in yeast cells.

Methods

Yeast culture and manipulation

All yeast analyses were performed in strains derived from (BY4741, *MAT*a; *his3Δ1*; *leu2Δ0*; *met15Δ0*; *ura3Δ0*). Growth, handling, and transformation of yeast involved standard techniques. HTP-tagged Nop1, Nop56, Nop58 and Mtr4 strains constructed in our lab in the background of BY4741 were previously described (Granneman *et al.*, 2009; Delan-Forino *et al.*, 2017). Oligonucleotides are listed in Supplementary Table 1.

Initial steps of yeast culture growing and UV crosslinking for CLASH are as previously described for CRAC (Tuck & Tollervey, 2013). In brief, yeast cultures were grown to OD_{600}=0.5 and crosslinked (254 nm, 100 s). For RNA sequencing three transformants of P_{GAL}*::SNR17A snr17BΔ* U3mut, snr4Δ, snr45Δ and snr78-78Δ were grown in YNB supplemented with Formedium CSM (complete or –Trp) and 2% w/v glucose. BY4741 was grown as a control. Cultures were grown from OD600 ~0.1 until they reached OD600 ~0.5, at which point all samples were pelleted by centrifugation at 4°C at 1940xg for 3min. "Standard" samples were resuspended in 1ml 1X PBS, then centrifuged and the pellets frozen. "Ice" samples were resuspended in 10ml 4°C 1X PBS and incubated for 20min on ice before being pelleted and frozen.

Construction of strains expressing mutant U3, strains with SNR4 and SNR45 depletion

U3 is encoded in *S. cerevisiae* by 2 redundant genes *SNR17A* and *SNR17B*. To assess U3 functions we deleted the *SNR17B* genetic locus and placed the expression of *SNR17A* under the control of a repressible P_{GAL} promoter. To create *kanMX6-*P_{GAL1}*-SNR17A snr17BΔ* strains, genetic manipulations were carried out in a standard manner as described (Longtine *et al.*, 1998) using corresponding pFA6a–MX6 plasmids. The *snr4::KanMX6* strains were created using similar methods.

Double snR4 snR45 depletion mutants were created with one snoRNA gene deleted and the other placed under P_{GAL1} transcriptional control. Primers oRP-063 –oRP066 (Supplementary Methods_d1) were used to PCR amplify pFA6a-His3MX6-PGAL1, and this was transformed into the reciprocal snoRNA deletion strain as described above, to create strains *HIS3MX6-*P_{GAL1}*-SNR4 snr45::KanMX6*, and *HISMX6-*P_{GAL1}*-SNR45 snr4::KanMX6*.

Primers used for snoRNA depletion:

SNR17B_dFP

GTAAAGAGGTAAGGATGTTAATATTGCCGTGGAAAA AATTGCAACGAGAGCGGATCCCCGGGTTAATTAA

SNR17B_dRP

ATTAAAATACTAAGTATAATGCGGCTCCAAAATACT
GAATCAAACCTTTGGAATTCGAGCTCGTTTAAAC

SNR4_delFP

TAGTTTTTTTGTCATTGATCTTTTCATTTTTTTATTTCA
AAATCCCCATCGGATCCCCGGGTTAATTAAG

SNR4_delRP

ACCCAGGTGAGACTGGATGCTCCATAGATTCCAAGATT-
TACGTAAGAATTGAATTCGAGCTCGTTTAAAC

To study U3 binding domains we generated a plasmid from which the truncated mutant U3 with deleted helixes 2 and 4 and helix 3 replaced with snR77 mRNA binding sequence was expressed under the endogenous promoter. Boxes B, C, C' and D were unaltered. The sequence containing the endogenous P_{SNR17A} promoter and mutant U3 flanked by XbaI and EcoRI restriction sites was cloned into pRS413 (centromeric, -His) plasmid (Frazer & O'Keefe, 2007) to obtain U3 mutant construct (U3mut). For complementation experiments we cloned the endogenous PSNR17A promoter and wild type SNR17A into the same vector (U3wt).

Sequence used to create U3mut expressing vector:

TATTTCTTTCTAGAGTTTCAAAAAAAATATTGATTCT
TTTTTTATAAAAATATCAGTAGTATGTATGGGCTGATT
GTATGGTTTATACAGGCCGTCAAAATTTTTTCACCCC
CCCATACCCCACATACCTTTTACTATTAACCCTGATT
TTTTTTCTTTTCACATACAGCGCCTTAAGGCGAAGGCA
AATCCTGAAAATTTTCTCATTTGCTTTCCCCCACCAG
ACATATATAAAGGCTTTGTATTCTGCTGTCAATTAGAT
TTAGTACATCTTTTCTCTTATGTTTTCTTCTTGTTTCT
ACTTAAAATCTGTGTCGACGTACTTCATAGGATCAT
TTCTATAGGAATCGTCACTCTTTGACTCTTCAAAAGAG
CCACTGAATCCAACTTGGTTGATGAGTCCCATAACCTTT
GTACCCCAGAGTGAGAAACCGGCGCGATGATCTTGA
ATATGATGATTATAACAAAAACAAGTTTTTGCTC
TAGTGGGTACAAATGGCAGTCTGACAAGTTAACCAC
TTTTTTCCTTTTCTAAATTGTTTAAAACCAAAGGTTTG
GTTTTCAGTTAAGAAATTGGATTAGTTGGTGTGTAAGT
ATAATTAAATGTAGTGAATTCATCATTTA

Three *kanMX6-*P_{GAL1}*::SNR17A snr17BΔ* clones containing pRS413(His)_U3mut plasmid were selected on –His SD medium. Cultures were grown in –His SD 2% Galactose overnight, then transferred to –His SD 2% Glucose, diluted to OD_{600}=0.1 and grown for 36 h to deplete the chromosomally expressed snoRNAs. Strains *HIS3MX6-*P_{GAL1}*-SNR4 snr45::KanMX6*, and *HISMX6-*P_{GAL1}*-SNR45 snr4::KanMX6* were depleted of corresponding snoRNAs in similar manner.

RNA isolation

Cells were harvested and total RNA was isolated using hot Phenol-GTC lysis. Briefly: cells were disrupted by vortexing with zirconium beads and proteins were denatured in GTC: Phenol pH4 (1:1) mixture for 5 min at 65°C. Chloroform:IAA (24:1) was added and, after centrifugation, the aqueous phase was collected. RNA was precipitated, resuspended in RNase free water and stored at -70°C. The quality and quantity of RNA preparation was assessed using an Agilent 2100 Bioanalyzer System with RNA Nano Chips and RNA 6000 Nano Reagents (Agilent Technologies).

Northern blotting for pre-rRNA analyses

A total of 5 µg or 10 µg of samples were combined with the recommended volume of glyoxal as per the protocol for the Ambion Northern Max-Gly Kit. Samples were electrophoresed on a 1.2% w/v agarose 1x BPTE (10 mM PIPES; 30 mM Bis-Tris; 1 mM EDTA) gel at 50 V overnight at 4°C in 1x BPTE buffer. The gel was treated for 20 min with 75 µM NaOH, followed by 20 min in 0.5 M Tris pH 7.5 plus 1.5 M NaCl. It was then washed with 6X SSC (0.5 M NaCl and 50 mM $Na_3C_6H5O_7$, pH 7) for 20min. RNA was transferred onto a GE Healthcare Hybond-N+ membrane overnight at room temperature by capillary transfer. RNA was immobilized on the membrane by UV cross-linking at 120 mJ cm^{-2}. Results of northern blotting are shown on figshare (Dudnakova *et al*., 2018).

The probes were labelled with [γ^{32}P]-ATP using T4 PNK (NEB) and hybridized overnight in 20X SSC (3M NaCl and 0.3 M sodium citrate, pH7) with Denhardt hybridization buffer (100x solution: 2% w/v Ficoll 400, 300 mM NaCl, 2% w/v Polyvinylpyrrolidone, 2% w/v BSA). The membrane was then exposed to a phosphor screen, the signal was detected using a fluorescent imaging analyzer (FLA-5000 scanner, Fujifilm).

RNASeq cDNA Library preparation

From total RNA samples (10 µg total RNA), poly(A)-tailed RNAs were selected using Dynabeads™ mRNA Purification Kit (Thermo Fisher Scientific) according to manufacturer's protocol. RNA-seq cDNA libraries were prepared with NEBNext® Ultra™ Directional RNA Library Prep Kit for Illumina according to the instruction manual provided (https://international.neb.com/-/media/catalog/datacards-or-manuals/manuale7420.pdf) using 50-100 ng Poly(A)-selected RNA samples as starting material. NEBNext Multiplex Oligos (NEB) adaptors and primers were used to multiplex cDNA Illumina libraries.

Quantitative PCR

Total RNA was DNase-treated as per the Ambion Turbo DNase protocol. RT was carried out from 0.5µg of treated RNA with a RETROscripts Reverse Transcriptase kit and Random decamer primers (Ambion). The RT sample was then diluted to either 1 ng $µl^{-1}$ or 0.1 ng $µl^{-1}$ and 4 µl was used with Takara Bio SYBR Premier Ex Taq 2x mix and the corresponding set of primers (Supplementary Document 3). This was then amplified by qPCR by the Agilent Stratagene Mx3005P, using the following method for SYBR Green with dissociation curve: 95°C for 1min, followed by 40 cycles (95°C for 15 s, 55°C for 15 s, and 72°C for 15 s), followed by 95°C for 1 min, 55°C for 30 s and 95°C for 30 s.

Crosslinking, preprocessing and aligning of Illumina sequence data

CLASH experiments using yeast cells were performed on cultures grown in synthetic dextrose (SD) medium with 2% glucose,

lacking Trp to OD600 0.5, or following to synthetic medium containing 2% v/v ethanol plus 2% v/v glycerol for 20 min. Actively growing cells were cross-linked in culture medium (Granneman *et al.*, 2011) and processed for CLASH as previously described (Granneman *et al.*, 2009; Helwak *et al.*, 2013; Kudla *et al.*, 2011). Briefly, cells were lysed in buffer "A" containing 50 mM Tris-HCl pH 7.8, 2 mM $MgCl_2$, 150 mM NaCl, 0.4% NP-40 (all chemicals acquired from Sigma-Aldrich) with RNAsin Ribonuclease Inhibitor (Promega). RNA-protein complexes were isolated by binding to an IgG column (GE), washed in buffer A and released by TEV (Promega) cleavage. RNAs were partially digested using RNaceIT Ribonuclease Cocktail (Agilent). RNA-protein complexes were bound in denaturing conditions (6M Guanidinium HCl in buffer A) to a nickel affinity column (Ni-NTA agarose, QIAGEN). RNA end processing, radiolabeling and linker ligation were performed on the nickel column. 3' linker ligation and simultaneous internal hybrid ligation (ssRNA Ligase I, NEB) was carried out without ATP in ligation buffer. Subsequently, complexes were eluted (200mM Imidazole, 100mM DTT) and resolved on NuPage 4–12% gradient gels (Invitrogen, Thermo Fisher Scientific) transferred to nitrocellulose (GE), identified by autoradiography and excised. The proteins were then digested with proteinase K (Roche) and the cDNA library was created and amplified from the acquired RNAs using RT-PCR (Superscript III RT, Invitrogen; LA Taq, TaKara). 5' linkers used to prepare libraries contain a barcode, enabling samples to be multiplexed for sequencing, and a random 3 nt sequence in order to remove PCR duplicates by collapsing identical sequences during data analysis.

3' linker

miRCat-33 linker (IDT) AppTGGAATTCTCGGGTGCCAAG/ddC/

5' linkers (barcode marked in bold, random nucleotides as N)

L5Aa invddT-ACACrGrArCrGrCrUrCrUrUrCrCrGrArUrCrUrN-rNrNr**UrArArGrC**-OH

L5Ab invddT-ACACrGrArCrGrCrUrCrUrUrCrCrGrArUrCrUrN-rNrNr**ArUrUrArGrC**-OH

L5Ac invddT-ACACrGrArCrGrCrUrCrUrUrCrCrGrArUrCrUrN-rNrNr**GrCrGrCrArGrC**-OH

L5Bb invddT-ACACrGrArCrGrCrUrCrUrUrCrCrGrArUrCrUrN-rNrNr**GrUrGrArGrC**-OH

L5Bc invddT-ACACrGrArCrGrCrUrCrUrUrCrCrGrArUrCrUrN-rNrNr**CrArCrUrArGrC**-OH

L5Bd invddT-ACACrGrArCrGrCrUrCrUrUrCrCrGrArUrCrUrN-rNrNr**UrCrUrCrUrArGrC**-OH

L5Ca invddT-ACACrGrArCrGrCrUrCrUrUrCrCrGrArUrCrUrN-rNrNr**CrUrArGrC**- OH

L5Cb invddT-ACACrGrArCrGrCrUrCrUrUrCrCrGrArUrCrUrN-rNrNr**GrGrArGrC**-OH

L5Cc invddT-ACACrGrArCrGrCrUrCrUrUrCrCrGrArUrCrUrN-rNrNr**ArCrTrCrArGrC**-OH

L5Cd invddT-ACACrGrArCrGrCrUrCrUrUrCrCrGrArUrCrUrN-rNrNr**GrArCrTrTrArGrC**-OH

PCR primers

miRCat-33 primer (IDT) CCTTGGCACCCGAGAATT primer for RT

PE_miRCat_PCR CAAGCAGAAGACGGCATACGAGATCG-GTCTCGGCATTCCTGGCCTTGGCACCCGAGAATTCC library amplification

P5 AATGATACGGCGACCACCGAGATCTACACTCTTTCCCT-ACACGACGCTCTTCCGATCT library amplification

RNA-IP for U3 mutations

Strains expressing chromosomally encoded HTP tagged Nop1 or Rrp9 and mutant U3 (expressed from the plasmid) were grown to OD_{600} 0.5, Cells were collected, lysed in buffer A and RNA protein complexes purified on the IgG column (materials as for CLASH, see above). RNA was extracted using Phenol/Chloroform and analyzed by Northern Blot using anti-U3 DNA oligo probe 5 ' –CTATAGAAATGATCC, as described previously (Dandekar & Tollervey, 1989).

For hybridization, 15 ml of 20X SSC (3 M NaCl and 0.3 M sodium citrate, pH7) was mixed with 2.5 ml 100X Denhardt hybridization buffer (2% w/v Ficoll 400, 300 mM NaCl, 2% w/v Polyvinylpyrrolidone, 2% w/v BSA) and 1.25 ml 20% w/v SDS. This was incubated at 50°C and filter-sterilized. This solution was added to the membrane in a plastic box, and incubated for 1h at 37°C with shaking. To make hybridization probes, 1µl (10U) of T4 polynucleotide kinase (PNK) was mixed with 1 µl oligo (at 10 µM), 1.5 µl 10X PNK buffer, 9 µl H_2O and 2.5 µl γ-ATP (^{32}P). This was incubated at 37°C for 40 min, then purified on a Roche Mini Quick Spin Oligo column by centrifugation at 1000 g for 1 min. The labelled probe was added to fresh hybridization buffer and incubated with the membrane overnight at 37°C. The membrane was subsequently washed with 6X SSC plus 0.1% w/v SDS at 37°C, a total of three times for 10 min each. The membrane was then exposed to a phosphor screen and the signal detected using a fluorescent imaging analyzer (FLA-5000 scanner, Fujifilm).

PolyA selection

To select for poly(A) tailed RNAs, the NEBNext poly(A) mRNA Magnetic Isolation Module kit was used, and the protocol followed. A total of 20 µl Oligo $d(T)_{25}$ beads per sample were washed twice with 100 µl 2x RNA Binding Buffer. RNA samples were DNase-treated with Promega 10X RQ1 buffer, 1 unit RQ1 DNase and 1 unit of Promega RNasin and incubated at room temperature for 30 min. The reaction was stopped by adding 50 mM EDTA and incubating on ice, followed by addition of 10 mM Tris pH7.8 and 100 mM NaOAc, and transfer into RNA Phenol:Chloroform:IAA (25:24:1), pH4. The RNA isolation protocol was followed from this step. A total of 2 µg

total RNA, as measured by Agilent Bioanalyzer RNA chip was diluted to a total of 50 µl in nuclease-free water. The beads were then resuspended in 2x RNA Binding Buffer and added to the RNA samples. The samples were heated at 65°C for 5 min then cooled to 4°C. This was then resuspended, incubated at room temperature for 5min, resuspended a second time and incubated a second time. The samples were placed on a magnetic rack and the supernatant discarded. Each sample was washed twice with Wash Buffer, then resuspended in 50 µl Tris Buffer and mixed. The samples were heated at 80°C for 2 min then cooled to 25°C and diluted with 2x RNA Binding Buffer. Samples were subsequently incubated at room temperature for 5 min, resuspended, and incubated again. These were then placed on the magnetic rack, and the supernatant discarded. Samples were washed with Wash Buffer, and all supernatant thoroughly removed and discarded. mRNA was eluted from the beads by adding 17 µl 10 mM Tris pH7.8 and incubating at 80°C for 2 min then held at 25°C. Samples were placed on the magnetic rack, and the supernatant transferred into a fresh tube. RNA concentration was measured by Agilent Bioanalyzer RNA chip and Thermo Fisher Qubit RNA HS (high sensitivity) Assay kit.

RNA library preparation for Illumina sequencing

50 ng poly(A)-selected mRNA was incubated with 5X NEBNext First Strand Synthesis Reaction Buffer and 1 µl NEBNext Random Primers in 10 µl total volume. The samples were incubated for 15min at 94°C, then cooled on ice. Added to this was 0.5µl Murine RNase Inhibitor, 0.1µg Actinomycin D, 1µl Protoscript II Reverse Transcriptase and 8.5µl nuclease-free H_2O. The samples were then incubated at 25°C for 10 min, 42°C for 15 min, then 70°C for 15 min. 10x Second Strand Synthesis buffer, 4 µl Second Strand Synthesis Enzyme mix and H_2O were added to the samples to a final volume of 80µl, and the tubes were incubated in a thermocycler for 1 h at 16°C. Samples were then purified using a QIAquick PCR purification kit as follows: 5 volumes of PB buffer were added to 1 volume of PCR reaction and mixed. The mixture was applied to a QIAquick column centrifuged at 16,250 g for 1min. The flow-through was discarded. 750 µl PE buffer was then added to the column and the column centrifuged as above, then the flow-through discarded. The column was then transferred to a fresh 1.5 ml Eppendorf and left with lid open for 5 min. This was centrifuged for 2min. The column was then transferred to a fresh 1.5 ml Eppendorf, 58 µl 10 mM Tris pH7.8 pipetted into the centre of the column and the column left to stand for 1 min. Samples were eluted by centrifugation for 1min and stored at -20°C overnight.

10x NEBNext End Repair Reaction Buffer and 3 µl NEBNext End Prep Enzyme Mix were added to the thawed purified double stranded cDNA. The samples were incubated at 25°C then 65°C for 30 min each, before cooling to 4°C. 15 µl Blunt/TA Ligase Master Mix and 1.5µM NEBNext Multiplex Adapter were added directly to the End Prep reaction mix along with nuclease-free water to make a total volume of 83.5 µl. Samples were mixed and incubated for 15 min at 20°C. The reactions were then purified using the QIAquick PCR purification kit as above. Samples were eluted in 20 µl 10 mM Tris pH7.8.

A total of 3 µl NEBNext USER enzyme, NEBNext Q5 2x Hot Start HiFi PCR Master Mix, 2.5 µl Universal PCR Primer and one 2.5 µl Index Primer per PCR reaction (1-9 for samples 1-9) were added to the 20 µl cDNA and mixed. Samples were subjected to PCR by the following method: 37°C for 15min, [98°C for 30 s, 98°C for 10 s, by 65°C for 75 s] for 12 cycles, 65°C for 5 min then held at 4°C. The PCR reactions were then purified using the QIAquick PCR purification kit. Samples were eluted in 18 µl in 10 mM Tris pH7.8. Each sample was purified on a 3% w/v MetaPhor agarose 1X TBE gel (Fisher Scientific 10X Tris/Borate/EDTA solution) with a Fisher Scientific exACTGene 50 bp Mini ladder and 1:10,000 Invitrogen SYBR safe DNA gel stain, until bromophenol blue had migrated the length of the gel. The band ranging between 150–200 bp was extracted. This was purified using the QIAquick Gel Extraction Kit as follows: 6 volumes of QG buffer were added to 1 volume of gel. This mix was incubated at 50°C for 10 min, vortexing occasionally. 1 volume of isopropanol was added and the mix inverted. This mix was applied to a MinElute column and centrifuged at 16,250 g for 1 min. The flow-through was discarded, and the remainder of the mix applied and centrifuged as above. The column was then washed with 500 µl QG buffer and the column centrifuged again, with flow-through discarded. 750µl PE buffer was then used to wash the column, followed by centrifugation of the column and transfer to a fresh 1.5ml Eppendorf. The column was left to dry for 5min, then centrifuged for 3 min. In a fresh 1.5 ml Eppendorf, 16 µl 10 mM Tris pH7.8 was added to the centre of the column, left to incubate for 2 min, then the cDNA eluted by a 1 min centrifugation. The quality of library was assessed by Agilent Bioanalyzer DNA chip and Thermo Fisher Qubit DNA HS Assay kit.

Quantitative PCR for mRNAs

RNA was measured by Thermo Scientific NanoDrop Spectrophotometer and DNase-treated as per the Ambion Turbo DNase protocol as follows: 10X TURBO DNase buffer and 2U TURBO DNase was added to 10µg RNA diluted in 45µl H2O. This was incubated at 37°C for 30 min, before adding 10X DNase Inactivation Reagent. This mix was incubated at room temperature for 5 min, mixing occasionally. The mix was then centrifuged at 9,250*g* for 1.5 min, before transferring the supernatant to a fresh tube. 0.5 µg of this was then used in RETROscript's Reverse Transcriptase kit. Random decamer primers or oligo(dT) primers were added to a final concentration of 5 µM and nuclease-free H2O added to a final volume of 12 µl. The sample was mixed and heated at 80°C for 3 min, then incubated briefly on ice. 10X RT (reverse transcription) buffer was added, together with 4 µl dNTP mix (2.5mM per dNTP), 10 U RNase Inhibitor, and 100 U Reverse Transcriptase. The sample was mixed and incubated at 42°C for 1 h, followed by 10 min at 92°C. The RT sample was then diluted to either 1 ng μl^{-1} or 0.1 ng μl^{-1}. 4 µl of this was mixed with 6 µl of: Takara Bio SYBR Premier Ex Taq 2 X mix, 50 X ROX reference dye and 10 µM of forward and reverse primers (final concentrations 1 X, 1 X and 0.2 µM, respectively). This was then amplified by qPCR by the Agilent Stratagene Mx3005P, using the following method for SYBR Green with dissociation curve: 95°C for

1 min, [95°C for 15 s, 55°C for 15 s, and 72°C for 15 s] for 40 cycles, followed by 95°C for 1 min, 55°C for 30 s and 95°C for 30 s. Primer sets were tested with a standard curve of genomic DNA before use with samples, and each primer set tested with a no-template mix in the qPCR. Each sample was run with a no-RT control of the same concentration to ensure DNA contamination was minimal. For a subset of qPCRs, samples were DNase-treated, then poly(A)+ selected. RNA from this was then used in the RT reaction, using random decamer primers or oligo(dT) primers. qPCR was carried out as described above.

Analysis of qPCR data for mRNAs

To determine the 2-ΔΔCt for each experiment technical replicates for both the test gene and *TAF10* were normalized to the corresponding replicate of added *Schizosaccharomyces pombe ACT1*, to account for experimental variance between samples. The test gene was then normalized to the non-target, housekeeping gene *TAF10*, and the average of each biological replicate taken. These were then normalized to the average of each BY4741 biological replicate, and a two-tailed homoscedastic t-test applied (two samples, equal variance). The difference between the Ct (threshold cycle) of *TAF10*) in the deletion strain was calculated, as was the difference between the Ct of the test gene and the housekeeping gene in the WT strain. The latter value was subtracted from the former to give the ΔΔCt value. The exponential of –ΔΔCt gave the relative expression of the test gene in the deletion strain. The average of 2-ΔΔCt replicates for each gene was taken to determine fold change (FC). A one-sample t-test was performed to test for statistical significance.

Bioinformatics

Analysis of yeast CLASH data

Raw sequences preprocessed prior to alignment using hyb version 0.0 (Travis *et al.*, 2014) running the hyb preprocess command with standard parameters. The preprocessed data were aligned to a custom database containing unspliced genes (with snoRNA genes extended by 20 bp in each direction and masked out of the genes in which they are contained where appropriate). A custom database was built using reference data from ensembl release 77. Alignment was performed using the blastall command, using the standard parameters from the hyb pipeline. The aligned reads were processed using a variant of the hyb pipeline, modified slightly to extract snoRNA hybrids rather than microRNA hybrids preferentially. Downstream analysis was performed on reproducible hybrids (in which both fragments were found to overlap in two or more hybrids) with a predicted folding energy of -12dG or below. The analysis was performed using hybtools version 0.3 (Dunn-Davies, 2018). Reference data for the analysis of yeast methylation sites were obtained from the snoPY database (Yoshihama *et al.*, 2013).

snoRNA alignment

NCBI BLASTn alignments of snoRNAs were performed using parameters: Expect threshold; 10: Word size; 11; Match/mismatch; 2, -3: Gap costs; existence 5, extension 2.

Analysis of RNA-Seq data

Raw reads were reverse complemented using FASTX-Toolkit version 0.0.14 (Gordon, 2010) and trimmed using Trimmomatic version 0.32 (Bolger *et al.*, 2014) , to remove Illumina adapters.

For the U3 depletion experiments, transcript level quantification was then performed using kallisto version 0.43.1 (Bray *et al.*, 2016), using a *Saccharomyces cerevisiae* transcript database built from Ensembl release 77. Finally, differential expression was quantified using sleuth version 0.29.0 (Pimentel *et al.*, 2017).

In the case of the snR4 depletion experiments, the trimmed reads were mapped against the *Saccharomyces cerevisiae* genome (Ensembl release 77) using STAR version 2.4.2 (Dobin *et al.*, 2013). Gene level read counts were then obtained using htseq-count, from HTSeq version 0.9.1 (Anders *et al.*, 2015), and differential expression analysis was performed using DESeq2 version 1.11 (Love *et al.*, 2014).

The results of the differential expression analyses of all of the depletion experiments were compared with mRNA targets of snoRNAs from the CLASH data.

Statistical analysis

Statistical tests to determine whether CLASH targets were significantly over-represented among differentially expressed genes in the RNA-Seq analysis were carried out using the chisq.test and fisher.test functions from the stats package in R version 3.4.0.

Sequence data

All sequence data from this study have been submitted to the NCBI Gene Expression Omnibus under accession numbers GSE114680 and GSE118369.

Results

snoRNA-rRNA interactions

The construction of yeast strains expressing tagged forms of the snoRNP proteins Nop1, Nop56 or Nop58 under the control of the endogenous promoters has previously been reported (Granneman *et al.*, 2009). The tagged constructs are the only form of these proteins in the cell and support wild-type growth, showing them to be functional. To identify potential novel snoRNA interactions we applied the CLASH technique (Helwak *et al.*, 2013; Kudla *et al.*, 2011). This involves crosslinking of RNA complexes with tagged proteins by UV in living cells, affinity purification of the RNP complexes under stringent conditions, ligation of linker adaptors in parallel with internal ligation of captured RNA fragments base paired to each other, isolation of RNA, including RNA hybrids, followed by reverse transcription and high-throughput sequencing of cDNA libraries (Figure 1A). We performed total of 26 independent experiments using protein-tagged Nop1, Nop56 or Nop58 as bait in *S. cerevisiae*.

Analyses of single hits for yeast Nop1 during growth in glucose medium showed that snoRNAs were most frequently recovered,

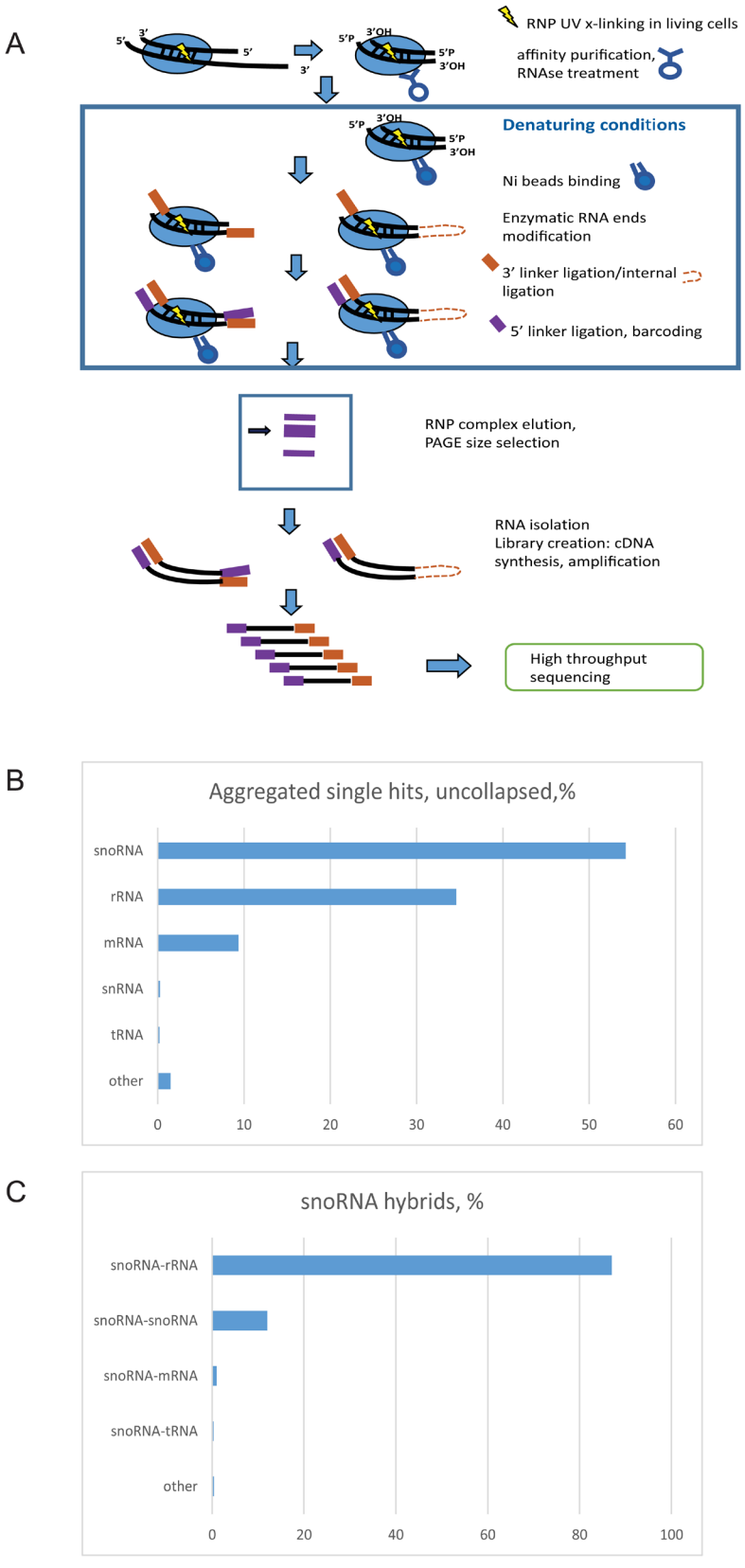

Figure 1. CLASH outline and results. (**A**) Scheme of the CLASH technique. Live cells were UV irradiated, crosslinked RNA–protein complexes extracted and affinity purified. In FLASH, purified complexes were crosslinked to the beads and subsequent steps carried out with denaturing washes. (**B**) Distribution of protein crosslinking sites by RNA type. (**C**) Distribution of chimeric reads involving snoRNAs, identified by CLASH and sorted by target RNA type.

both for pooled reads (Figure 1B) and individual proteins (Supplementary Figure 1A–C) followed by rRNA and mRNA. In contrast, for Nop56 and Nop58, rRNA sites were most frequently recovered. Recovered sequences that could be confidently mapped to two distinct regions of the genome (see Methods) were regarded as representing chimeric cDNAs resulting from RNA-RNA ligation.

In total, we recovered 241,420 distinct hybrids in yeast, of which 123,642 were snoRNA-rRNA hybrids. Within our dataset, we found snoRNA-rRNA hybrids for all of the 43 C/D box snoRNAs reported to methylate yeast rRNA in the snOPY database (Yoshihama *et al.*, 2013). For 42 of these snoRNAs (all except snR65), hybrids were present in the dataset that overlapped each of the reported methylation sites in rRNA associated with the relevant snoRNA (Figure 2). For comparison, we reanalyzed our previously published data (Kudla *et al.*, 2011) using the same pipeline (Supplementary Figure 2).

In silico folding of the hybrid sequences using the ViennaRNA package (Lorenz *et al.*, 2011) was used to predict the stability of the base-paired interaction that gave rise to the hybrid. In order to identify stable, base-paired interactions, only chimeric sequences with a predicted ΔG of less than -12 kcal mol^{-1} were retained for analysis. Non-identical chimeric sequences, or sequences recovered from different analyses, in which both segments overlapped were regarded as demonstrating independent recovery of the same interaction. Only interactions supported by at least two independent sequences with a predicted ΔG of less than -12 kcal mol^{-1} were considered stable and reproducible, and further analyzed. A total of 190,597 hybrids passed these filters, of which 117,047 were snoRNA-rRNA hybrids.

From the set of reproducible hybrids, 87% of the snoRNA-interacting sequences were mapped to the rDNA, 12% to another snoRNA, 1% to mRNAs and 0.4% to other RNA species (Figure 1C). It is notable that some highly abundant RNA species were recovered at low levels, particularly tRNAs (0.2% of total hybrids or 0.3% of snoRNA hybrids before filtering), supporting the specificity of the interactions. The predominant recovery of snoRNA-rRNA interactions is in agreement with the known function of snoRNAs in ribosome synthesis.

On the 35S pre-rRNA sequence, 116,611 stable, reproducible chimeras between snoRNAs and the 18S, 5.8S or 25S rRNA were mapped to 601 high confidence interaction sites. Inspection of the locations of snoRNA-rRNA hybrids showed colocalization with snoRNA-directed methylation sites along the mature 18S and 25S rRNA (shown in grey in Figure 3A). Low signals were seen over the transcribed spacer regions and 5.8S rRNA, which lack methylation sites. Comparing to the known sites of rRNA methylation, we identified high-confidence, cognate snoRNA-rRNA hybrids that overlapped 51 of the 55 reported methylation sites, involving 40 of the 43 methylation guide C/D box snoRNAs; shown for snR128 (U14) and snR55 (Figure 3B, C). In total, 10 yeast snoRNAs gave rise to 66% of reproducible rRNA hybrids; snR128 (U14), snR60, snR55, snR40, snR48, snR76, snR24, snR17 (U3), and snR79. Reported methylation guide snoRNAs for which we did not find stable, reproducible snoRNA-rRNA hybrids were snR53, snR65, and snR78 (Figure 2A and Supplementary Table 2). A total of 53% of hybrids overlapping methylation site showed interaction pattern that supports methylation of the target nucleotide in rRNA (Supplementary Table 2).

We also observed many examples of interactions in which methylation sites are bound by non-cognate snoRNAs that would be predicted to block methylation guide function. It is possible that competition between snoRNAs can exert additional level of regulation of ribosome modification (Supplementary Table 2). All methylation sites in the yeast rRNA have been confidently mapped (Taoka *et al.*, 2016; Yang *et al.*, 2016), making it unlikely that blocking interactions correspond to unknown methylation sites, at least under standard lab growth conditions.

Under conditions of reduced growth, the rate of ribosome synthesis is also reduced. To assess whether this was associated with altered snoRNA interactions, crosslinking was preformed following transfer of cells from glucose medium to medium containing 2% ethanol + 2% glycerol as sole carbon sources for 20 min. Some snoRNAs indeed displayed different binding pattern under different growth conditions (shown for snR4 in Supplementary Figure 3). Values for the growth of strains in different growth media is available on figshare (Dudnakova *et al.*, 2018).

A small number of yeast box C/D snoRNAs are not implicated in rRNA methylation and hybrids with the rRNA were also recovered for these species (Figure 3B). These are U3 (encoded by the genes *SNR17A* and *SNR17B*), snR4 and snR45. U14 (encoded by *SNR128*) has two characterized sites of interaction; the sequence flanking box D directs methylation, while base-pairing of the sequence flanking box D' is required for early pre-rRNA processing. We recovered snR17(U3) interactions with 18S as previously described (Kudla *et al.*, 2011). U3 interacted with pseudoknot region of rRNA via its region located immediately upstream of the D box sequence and partially in the helix 3 (Supplementary Figure 4). Earlier studies on U3 snoRNA structure and function showed that conserved boxes A, A', B, C, C' and D are important for U3 function in rRNA maturation. In contrast, helixes 2, 3, 4 were reported to be non-essential for U3 stability and function, although the essential protein Rrp9 binds to helixes 2 and 3 (Samarsky & Fournier, 1998; Venema *et al.*, 2000).

We recovered multiple hybrids between these helixes and the 35S pre-rRNA (Supplementary Figure 4 and Supplementary Table 2). The snoRNAs U3 and U3b are functionally redundant but essential for growth and pre-rRNA processing. To allow functional assays of U3, we deleted the *SNR17B* genetic locus and placed the expression of *SNR17A* under the control of a repressible P_{GAL} promoter. For complementation tests, we generated a plasmid expressing the truncated mutant U3 under the endogenous promoter. Helixes 2 and 4 of wild-type U3 snoRNA were deleted and the region of mRNA interaction in the helix 3 was replaced with snR77 mRNA binding sequence (Figure 4A). Analysis of a strain lacking the cluster genes, *SNR72-SNR78* (see Materials and Methods), showed no clear alterations in

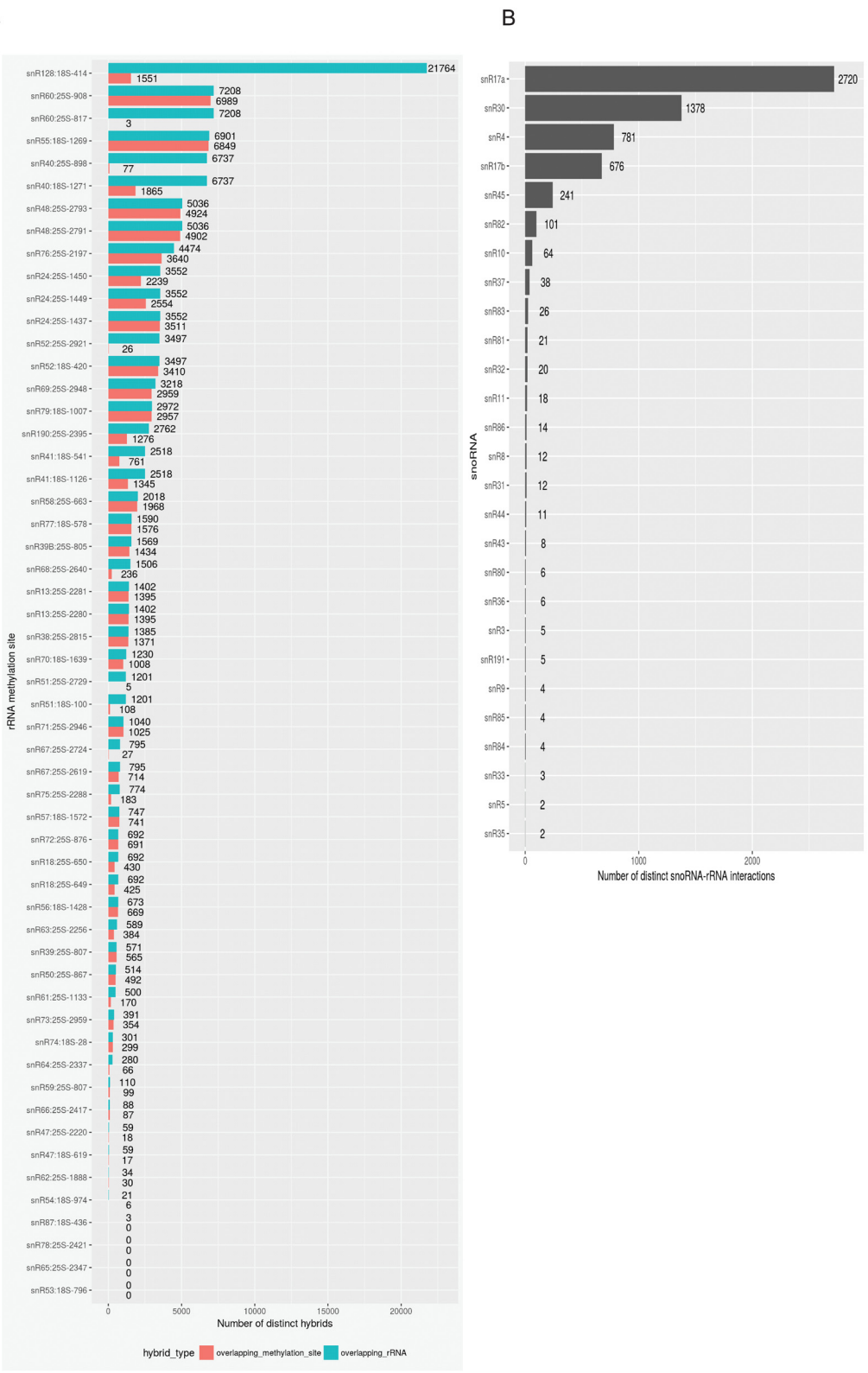

Figure 2. Numbers of snoRNA-rRNA interactions at sites of 2'-*O*-methylation. (**A**) All non-identical snoRNA-rRNA interactions overlapping each site of 2'-*O*-methylation in rRNA were tabulated. For each methylation site, numbers are indicated separately for snoRNA interactions overlapping the methylation site (upper green bar) and interactions predicted to guide methylation (lower red bars). (**B**) All non-identical snoRNA-rRNA interactions not overlapping 2'-*O*-methylation sites in the rRNA were tabulated. Note that none of the top scoring snoRNAs are expected to direct methylation.

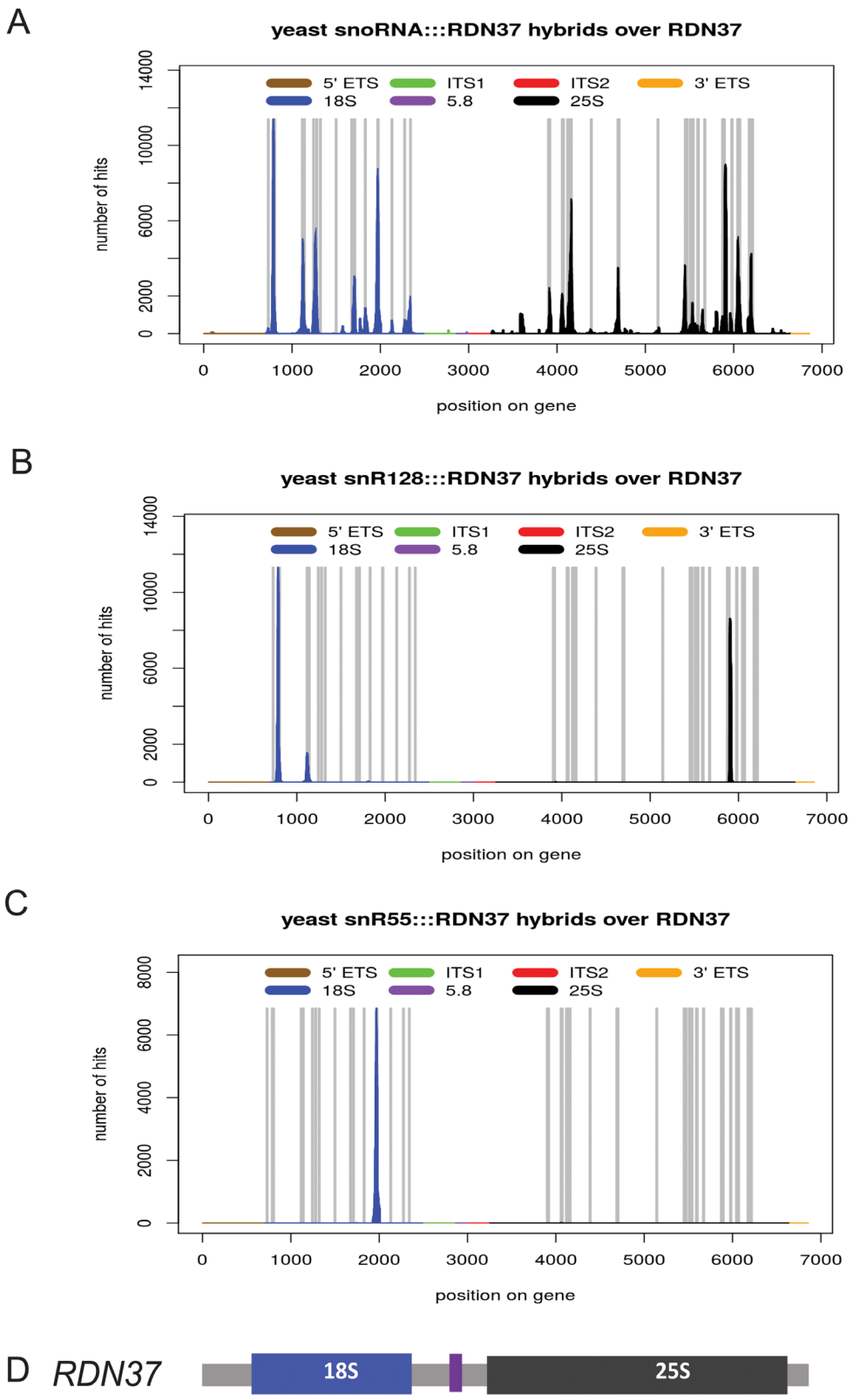

Figure 3. Distribution of snoRNA interactions on the rRNAs. Chimeric cDNAs between snoRNA sequences and the pre-rRNAs were identified by mapping to the rDNA locus *RDN37* and the number of hybrid hits for each location was plotted. The peaks were located preferentially in the regions of known methylation sites and structural interactions. (**A**) All snoRNA-rRNA chimeras mapped to the rDNA. Vertical bars in grey indicate the sites of rRNA 2'-*O*-methylation. (**B**) Distribution chimeric reads involving snR128 (U14). (**C**) Distribution chimeric reads involving snR55. (**D**) Schematic of the rDNA locus, indicating the locations of the rRNA genes.

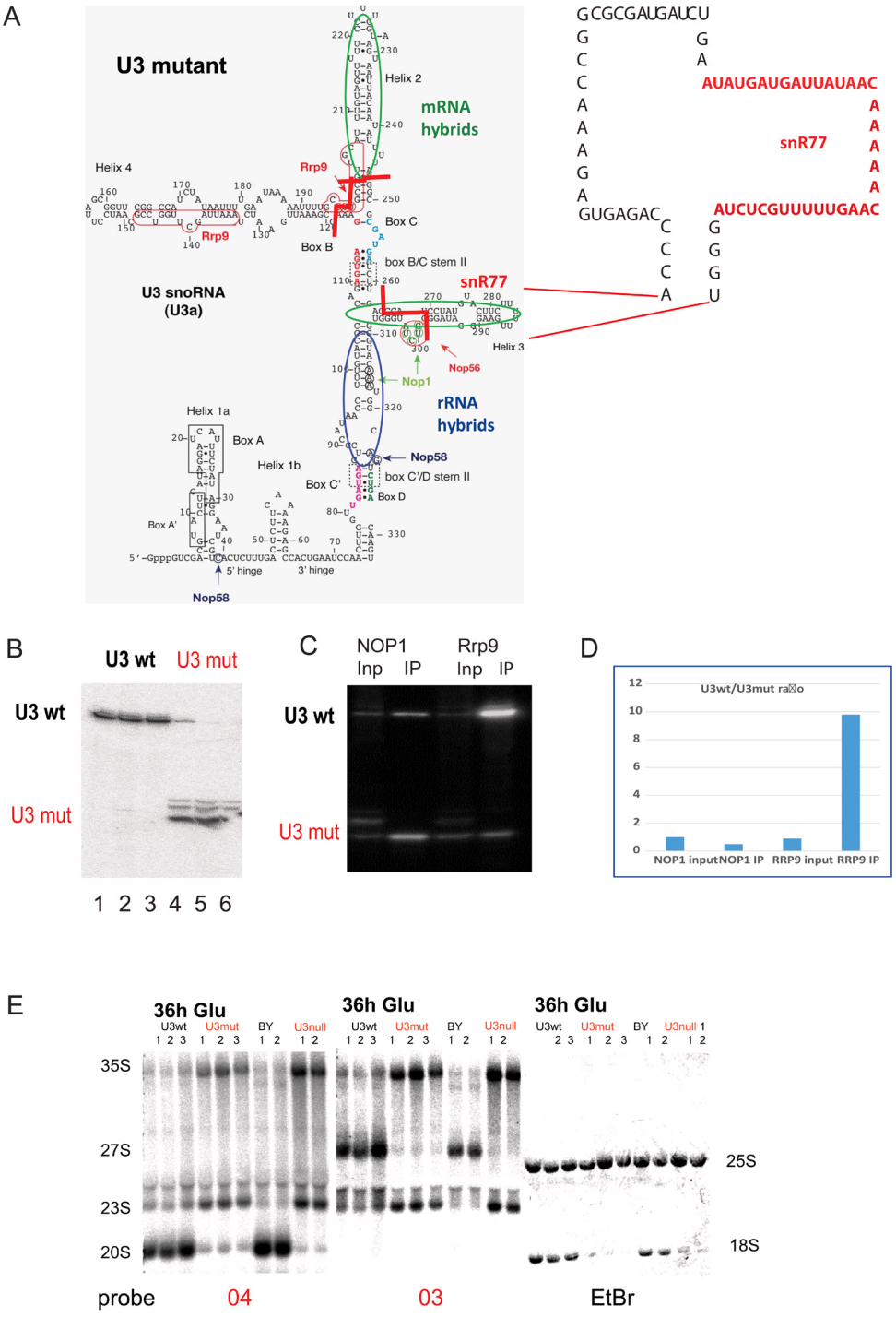

Figure 4. Effects of U3 mutations on pre-rRNA processing. (**A**) Left: Predicted structure of U3A. Regions forming hybrids with the rRNA identified by CLASH are circled in blue. Regions forming hybrids with mRNAs are circled in green. End points of deletions are indicated with red lines. Major crosslinking sites for snoRNP proteins are indicated with arrows and nucleotides are circled. Right: Structure of U3 deletion construct. Regions deleted or substituted with the snR77 sequence are indicated with dotted lines. (**B**) Northern blot showing expression of the wild type (U3 wt) and the truncated U3 (U3 mut). Lanes 1–3 and 4–6 show biological triplicates. (**C**) RNA IP northern blot from the strains expressing either TAP-Nop1 or TAP-Rrp9 and mutant U3. (**D**) Quantification of RNA IP. Signal densitometry of the selected lanes were measured with AIDA Image Analyzer v.4.15 densitometry software and plotted. (**E**) Northern analysis of pre-rRNA processing following transfer of the U3mutant strain to glucose medium for 36 h. U3 strains have endogenous U3 expression under P_{GAL} control, complemented by plasmid expression of wild type U3 (U3 wt lane) or the truncated mutant (U3mut lanes). As controls, the parental strain (BY) and the non-complemented (U3null lanes) strains are shown. Lanes 1–3 or 1 and 2 for each sample show biological replicates. Site A2 is the 3' end of the 20S pre-rRNA and the 5' end of 27SA and 27SB pre-rRNAs. Probe 03 is located in the ITS1 region of the pre-rRNA, 3' to cleavage site A2. Probe 04 is located in the ITS1 region 5' to site A2.

mRNA levels, making snR77 appear a suitable sequence donor. U3mut was expressed under the control of the native P_{SNR17A} promoter in a strain carrying P_{GAL}*::SNR17A, snr17bΔ*, which conditionally expresses U3a under control of a galactose-inducible promoter and lacks U3b. In galactose medium, mutant U3m was stable and expressed at the levels comparable with endogenous U3a (Figure 4B and Dudnakova *et al.*, 2018). Following transfer to glucose to deplete endogenous U3, the strain was inviable (Supplementary Figure 4) in contrast to the previous report (Samarsky & Fournier, 1998). Maturation of 18S rRNA was inhibited, with accumulation of 23S and 27SA2 pre-rRNA (Figure 4E). This phenotype reflects inhibition of pre-rRNA cleavage at sites A_0, A_1 and A_2, and is characteristic of the effects of loss of U3 or U3-associated proteins, including Rrp9 (Venema *et al.*, 2000; Zhang *et al.*, 2013). Rrp9 was shown to interact with U3 in the helix 2 and 4 regions, and box C was shown to be important for Rrp9 binding. We propose that U3 binding is needed to tether Rrp9 to the pre-ribosome during maturation. This suggestion was supported by RNA-immunoprecipitation (Figure 4C, D) showing that Rrp9 was unable to bind the mutant U3, whereas Nop1 binding was similar for mutant and wild type U3.

Targets for snR4 and snR45

The non-essential snoRNAs snR4 and snR45 were not known to play any role in ribosome synthesis when these analyses commenced. Strains carrying *snr4Δ* or *snr45Δ* showed no detectable growth defect relative to the isogenic wild-type (Supplementary Figure 5A and Dudnakova *et al.*, 2018). As snR4 and snR45 were the only snoRNAs whose deletion did not impact on ribosome synthesis, it seemed feasible that they might have redundant functions, and we therefore generated double mutant strains carrying *HISMX6-*P_{GAL1}*::SNR45 snr4Δ* and *HISMX6-PGAL1-SNR4 snr45Δ*. However, growth of the double mutant strain on glucose medium to deplete the GAL-regulated snoRNA did not confer a detectable growth phenotype (Supplementary Figure 5A).

To test for evolutionary conservation, the *SNR4* and *SNR45* sequences were analyzed using NCBI BLAST, optimizing for somewhat dissimilar sequences (blastn). A block of ~200nt was identified around the synonymous regions from distantly related fungal genomes and aligned using the MultAlin online alignment tool (Corpet, 1988). *SNR45* shows regions of conservation to fungal homologues and human U13 (SNORD13) (Supplementary Figure 5). Conservation was high over the 5' region, box C (nts 28-34), box D' (nts 97-100), box C' (nts 108-114) and box D (nts 193-196). However, the regions flanking box D and D', which would be the expected locations of the methylation guide were poorly conserved, whereas a well-conserved region was identified, spanning nts 140-151 (Supplementary Figure 6).

Comparison of *SNR4* to fungal homologues (Supplementary Figure 6) showed around box C (nts 15-21). Box C' is also highly conserved (nts 123-129) but no clear D' box, was identified. Box D is well conserved at nucleotides 184-187. A further well-conserved region was noted (nts 146-155), which does not correspond to known structural features or the expected location of a methylation guide sequence.

While this work was underway, it was reported that snR4 and snR45 direct 18S rRNA acetylation, at positions m5C1280 and m5C1773, respectively (Sharma *et al.*, 2015; Sharma *et al.*, 2017). Analysis of the CLASH data identified hybrids between snR4 and snR45 and sequences flanking the acetylated residues. For snR45, we recovered two snR45 hybrids with the sequence flanking ac^{4}C1773 (Supplementary Figure 5). The nucleotides involved in base-pairing correspond to the region high conservation noted in snR45 homologues. Notably, in analyses of human snoRNAs (manuscript in preparation), we identified a homologous interaction between U13 and the corresponding methylation site Ac1842 (Supplementary Figure 5).

Supplementary Figure 6 shows two examples of the 17 hybrids found between snR4 and this the region of 18S rRNA upstream of the ac^{4}C1280 (ΔG -13.8). The nucleotides involved in base-pairing corresponded to the region of high conservation between fungal snR4 homologues. Even using this region of conservation, no clear human homologue could be identified for snR4.

Mtr4 is associated with non-cognate snoRNA interactions

Many apparently stable (i.e. ΔG < -12 kcal mol^{-1}) snoRNA interactions were recovered at rRNA sites not predicted to guide methylation. Mtr4 is a 3'-5' RNA helicase and cofactor for the nuclear exosome complex, which appeared to be candidate factor that might participate in displacing snoRNAs from the pre-rRNA, particularly those bound at inappropriate locations. We therefore generated CLASH data for Mtr4-HTP (Delan-Forino *et al.*, 2017). Single hits from Mtr4 CLASH demonstrated the binding profile consistent with the known role of Mtr4 in pre-rRNA processing and previous results (Figure 5A) (Delan-Forino *et al.*, 2017). Mapping snoRNA hybrid hits on the pre-rRNA showed that most chimeras recovered overlapped known methylation sites (Figure 5B). Strikingly, however, when analyzed individually, the snoRNA binding profiles predominately do not show the expected binding pattern for methylation guide interactions. Chimeras recovered with Mtr4 and predicted to correctly guide methylation constituted only 7.2% of all hybrids overlapping methylation sites (Figure 5C, D), in contrast to 53% for Nop1, Nop56 and Nop58.

We propose that snoRNA docking at non-cognate sites is common, but is specifically relieved by the activity of Mtr4.

snoRNA-snoRNA interactions

Numerous stable, reproducible snoRNA-snoRNA hybrids (15,736) were identified. The majority represented snoRNA intermolecular stems, which reveal potential information on snoRNA secondary structure. In addition, 2,734 hybrids represented interactions between different box C/D snoRNAs, including 78 different snoRNA-snoRNA combinations.

Interactions were also identified between mature snoRNA sequences and the 5' and 3' flanking regions. These presumably occur within the snoRNA precursors and potentially function during snoRNP biogenesis (Figure 6). Notably, the region 70 nt 3' to the mature snoRNA was a strongly favored target, both for presumed interactions in *cis* within the pre-snoRNA and in *trans* with other snoRNAs. These positions potentially represent

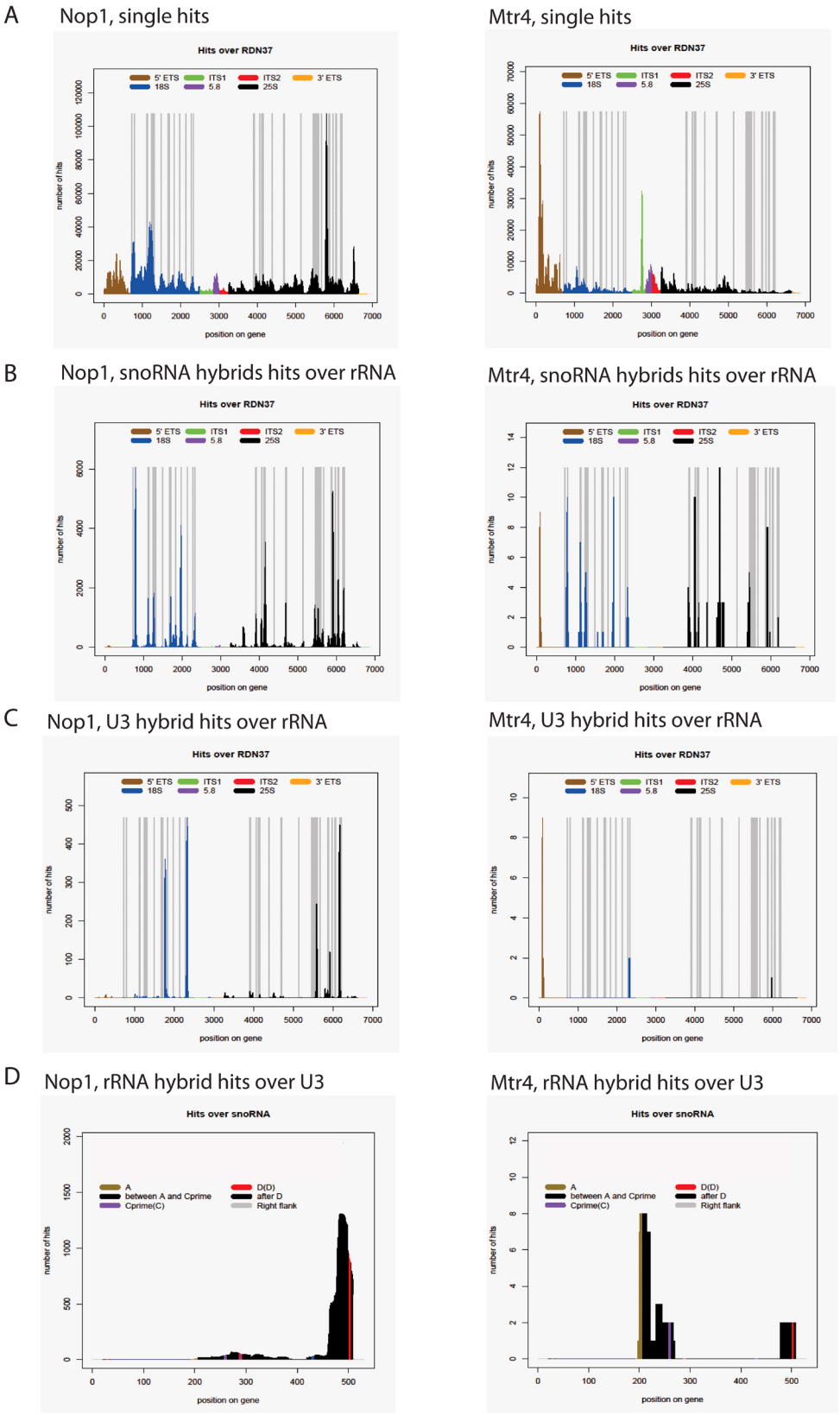

Figure 5. Comparison of snoRNA-rRNA interactions obtained in NOP1 and MTR4 CLASH. NOP1 CLASH data shown on the left, MTR4 CLASH data shown on the right. (**A**) Single hits mapped to the rDNA. (**B**) All snoRNA chimeras mapped to the rDNA. Vertical bars in grey indicate the sites of rRNA 2'-*O*-methylation. (**C**) Distribution chimeric reads involving snR17A/snR17B (U3). (**D**) Distribution of RDN37 chimeric reads over the *SNR17A* gene.

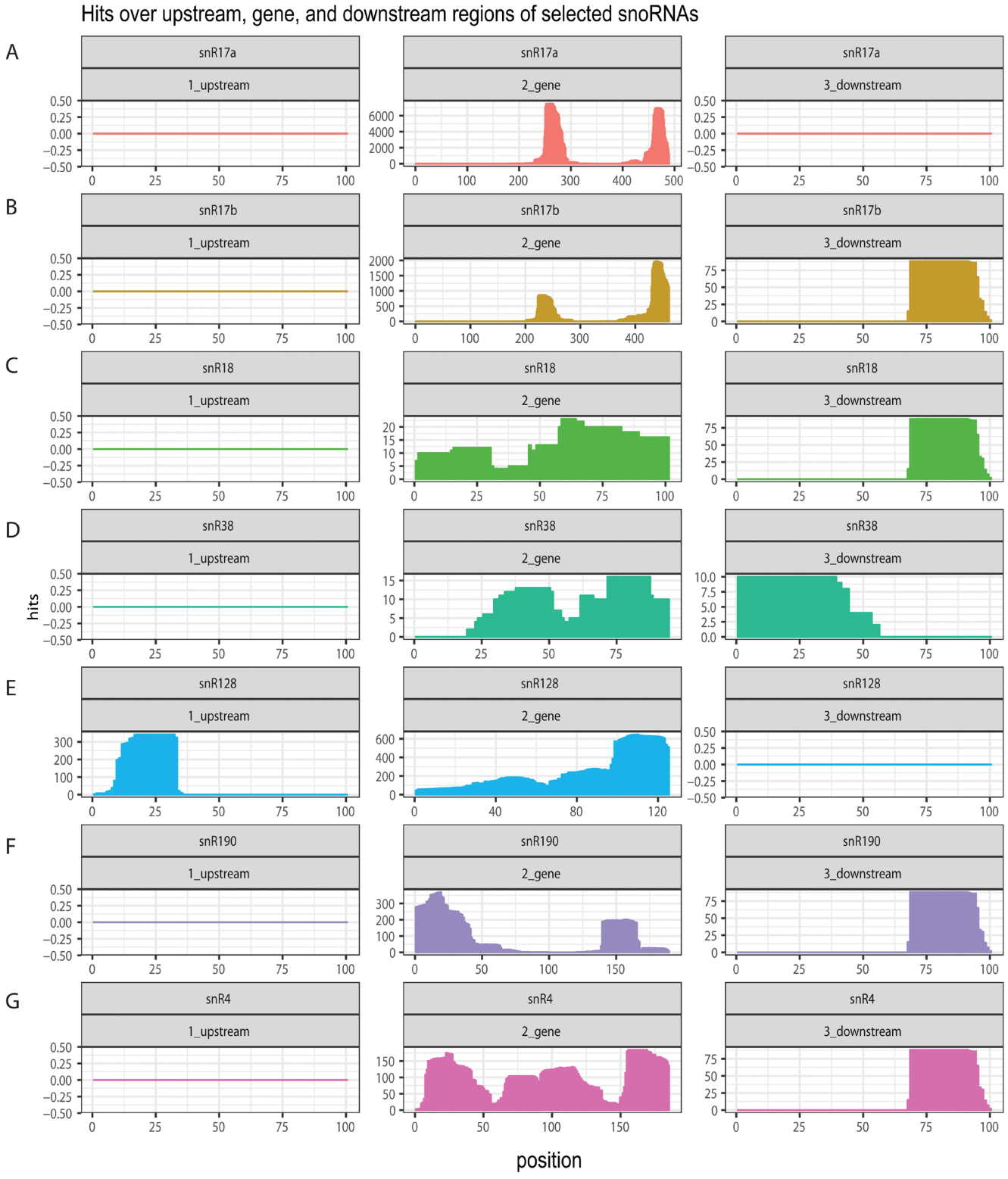

Figure 6. Distribution of snoRNA hits over the corresponding snoRNA genetic locus. Chimeric snoRNA-snoRNA cDNAs were mapped onto the genetic locus containing the snoRNA gene with 100bp upstream and downstream regions; the number of hybrid hits for each position was plotted. (**A**) snR17a; (**B**) snR17B; (**C**) snR18; (**D**) snR38; (**E**) snR128 (U14); (**F**) snR190; (**G**) snR4.

important regulatory sites that are presented for RNA binding. We noted that the pattern was different for snR128, potentially related to its production from a bicistronic precursor with snR190. Based on these finding we speculate the existence of regulatory loops, particularly in snoRNA biogenesis.

snoRNA-mRNA interactions

A potentially significant class of snoRNA chimeras involved snoRNA-mRNA interactions, which constituted 1.9% of all chimeric reads. These included 1,368 reproducible hybrids that represented 448 distinct interactions involving 39 snoRNAs and 382 mRNAs. Only hybrids with energy of interaction dG <-12 kcal mol^{-1} and independently recovered at least twice were included in analyses. Analyzing the distribution of reproducible snoRNA interactions across gene features identified 105 sites in 5' UTRs, 1276 sites in coding sequences, 32 sites in introns and 61 sites in 3'UTRs (Figure 7). Five snoRNAs (snR190, snR17a/b (U3), snR128 (U14), snR76, snR40) formed 63% of the recovered mRNA hybrids. Hybrids were also frequently recovered with snR39B and the orphan snoRNAs snR4 and snR45. Notably, several snoRNAs interacted with mRNAs via regions that were distinct from the rRNA binding sites (shown for snR128 (U14) in Figure 7). The filtered list of stable, reproducible snoRNA-mRNA interactions is presented in Supplementary Table 3; the complete list of interactions and sites is given in Supplementary Table 4.

Most snoRNA-mRNA duplexes are predicted to represent "structural" interactions that do not direct RNA methylation. However, we discovered 15 snoRNA-mRNA interactions that potentially promote methylation of target mRNAs (Supplementary Table 5).

We observed a correlation between hybrid and single mRNA hits, supporting the specificity and relevance of the hybrids (Supplementary Figure 7; see Pearson correlation between hybrid and single hits). In contrast, there was no clear correlation between mRNA expression level and presence in snoRNA hybrids (Supplementary Figure 7). These findings support the conclusion that the RNA-RNA chimeras recovered represent *in vivo* interactions.

Depletion of U3

A strain carrying P_{GAL}1*::SNR17A, snr17b*Δ, was transferred to glucose medium for 36 h to deplete U3. Changes in mRNA abundance were assessed by RNA-seq with NEBNext kit using a RiboMinus system to deplete rRNA from the samples. Sequence reads were mapped to the yeast genome and changes were quantified using DeSeq2 and Kallisto (see Methods).

The mRNA expression profiles obtained for U3 depletion were compared to CLASH data, to determine whether mRNAs showing altered abundance following snoRNA mutation are enriched for direct binding targets (Figure 8A). Most mRNAs showing altered abundance were not U3 CLASH targets, although these were significantly over-represented (red dots in Figure 8A) (Chi Square Test; P<0.05). In addition, mRNA targets of snoRNAs other than U3 were also altered in the U3 strain (red dots in Figure 8B). This might reflect the finding that the mutant U3 does not support ribosome biogenesis and 35S pre-rRNA is accumulated. This might act as a sponge, leading to snoRNA sequestration on the pre-rRNA and reduced availability for mRNA binding. At the same time, snoRNAs acting in the later stages of ribosome biogenesis might show reduced rRNA binding, potentially freeing them to bind non-ribosomal targets.

Depletion of snR4

To assess potential roles for snR4 in mRNA expression or stability, the *SNR4* gene was deleted from strain BY4741. The effects of *snr4Δ* on mRNA levels were assessed under normal growth conditions of SD (glucose) medium at 30°C (Figure 9A) and following stress induced by brief transfer to ice-cold PBS (Figure 9B); the conditions used for initially reported snoRNA CLASH analyses (Kudla *et al.*, 2011). RNA abundance was assessed by RNA-seq as described for the U3 mutant strain.

As for U3, most mRNAs showing apparently altered abundance were not snR4 CLASH targets. However, there was a statistically significant (Fisher's exact test; P <0.05) over-representation of mRNAs identified as interacting with snR4 in CLASH analyses among species showing altered accumulation in *snr4Δ* strains, both during normal growth and following stress (Figure 9A, B). RNAs showing both altered expression in *snr4Δ* and recovery as snR4-mRNA hybrids were enriched in GO terms for genes involved in metabolic processes. These data suggest a possible role of snR4 in stress response, which would be consistent with differences in snR4 binding to rRNA in normal growth and stress conditions.

Selected snR4 CLASH targets that were also found to be altered in abundance by RNA-seq were further tested by RT-qPCR (Figure 9C). Consistent with RNA-seq data, mRNAs abundances were reduced in strains lacking snR4 and showed greater effects following transfer to cold PBS than during exponential growth on glucose medium. The effects were statistically significant, but of low magnitude. Figure 9C shows the relative fold changes for the three snR4 CLASH targets and *RCK1* along the y axis, compared to WT. The red dashed line indicates a fold change of 1, showing the WT normalized expression for each gene. In standard conditions upon *SNR4* deletion, *ALD6* had a fold change of 1.54. This matched the direction of the fold change of 2.0 shown in poly(A)$^+$ selected RNA sequencing. *RCK1* showed a fold change of 2.4, which was similar to the 2.8 fold change observed in RNA sequencing. Both *ALD6* and *RCK1* had statistically significant differential expression upon *SNR4* deletion, with p values of 0.019 and 0.002, respectively. The negative control *RPS20* showed a fold change of 0.83 by qPCR, which is comparable to its fold change of 0.874 from RNA sequencing. However, the p value was 0.091, which is not significant. Similarly, *TMA7* showed a fold change of 0.860 in RNA sequencing, but had a fold change of 0.96 in qPCRs, with a p value of 0.75. Full Ct values obtained from RT-qPCR are available on figshare (Dudnakova *et al.*, 2018).

Discussion

We report the systematic analysis of yeast snoRNA interactions, by CLASH analyses using tagged forms of the major

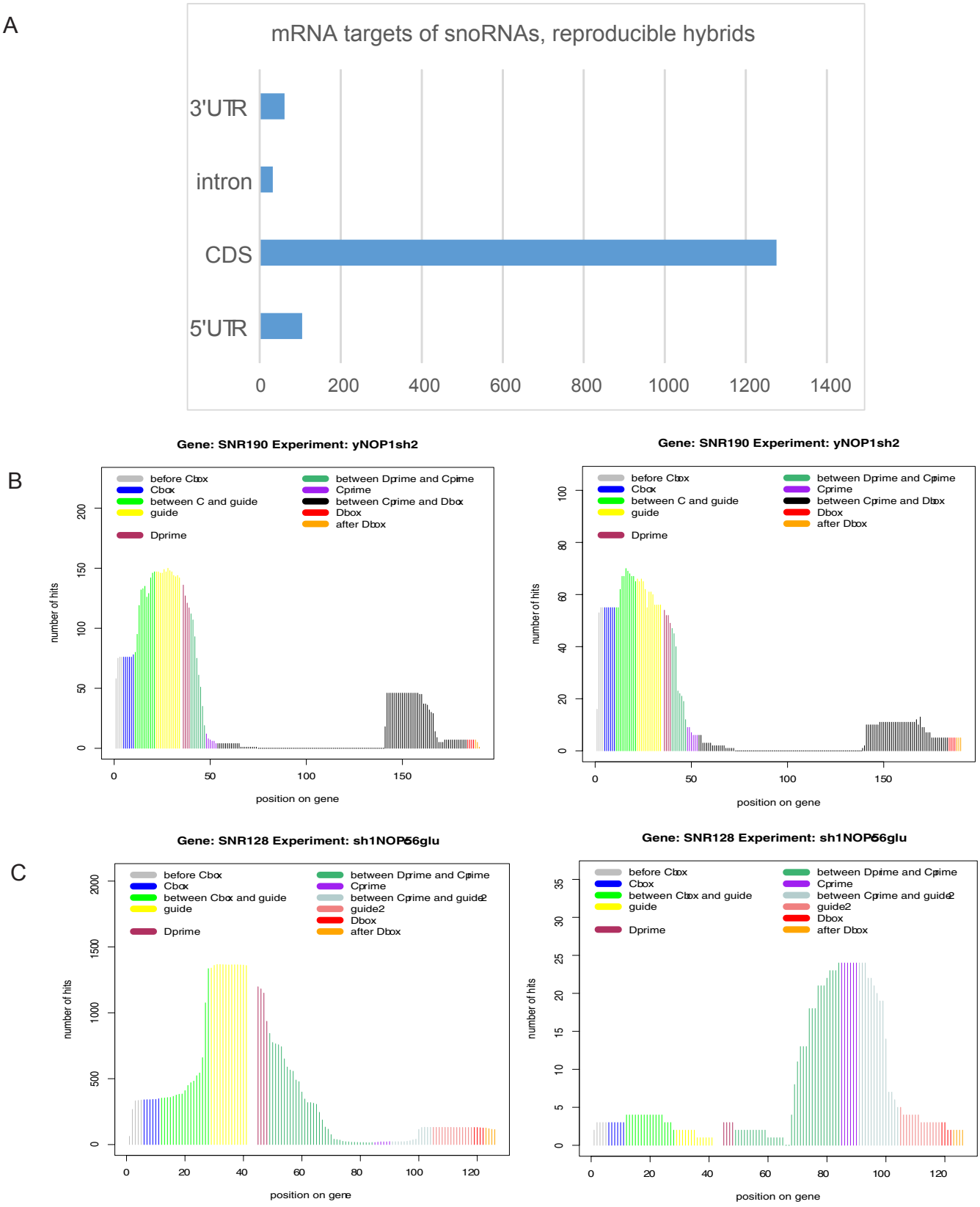

Figure 7. snoRNA-mRNA interactions. (**A**) Distribution of snoRNA hits over mRNA features. Chimeric cDNAs between snoRNA sequences and the mRNA sequences were identified by mapping to the yeast genome (ensembl release 77; see Methods) followed by allocation to the annotated mRNA features. The number of snoRNA hybrids involving mRNA UTRs, exons or introns was plotted. (**B**) Hybrid hits involving rRNA (left) and mRNA (right) hits plotted over snR190. (**C**) Hybrid hits involving rRNA (left) and mRNA (right) hits plotted over snR128 (U14).

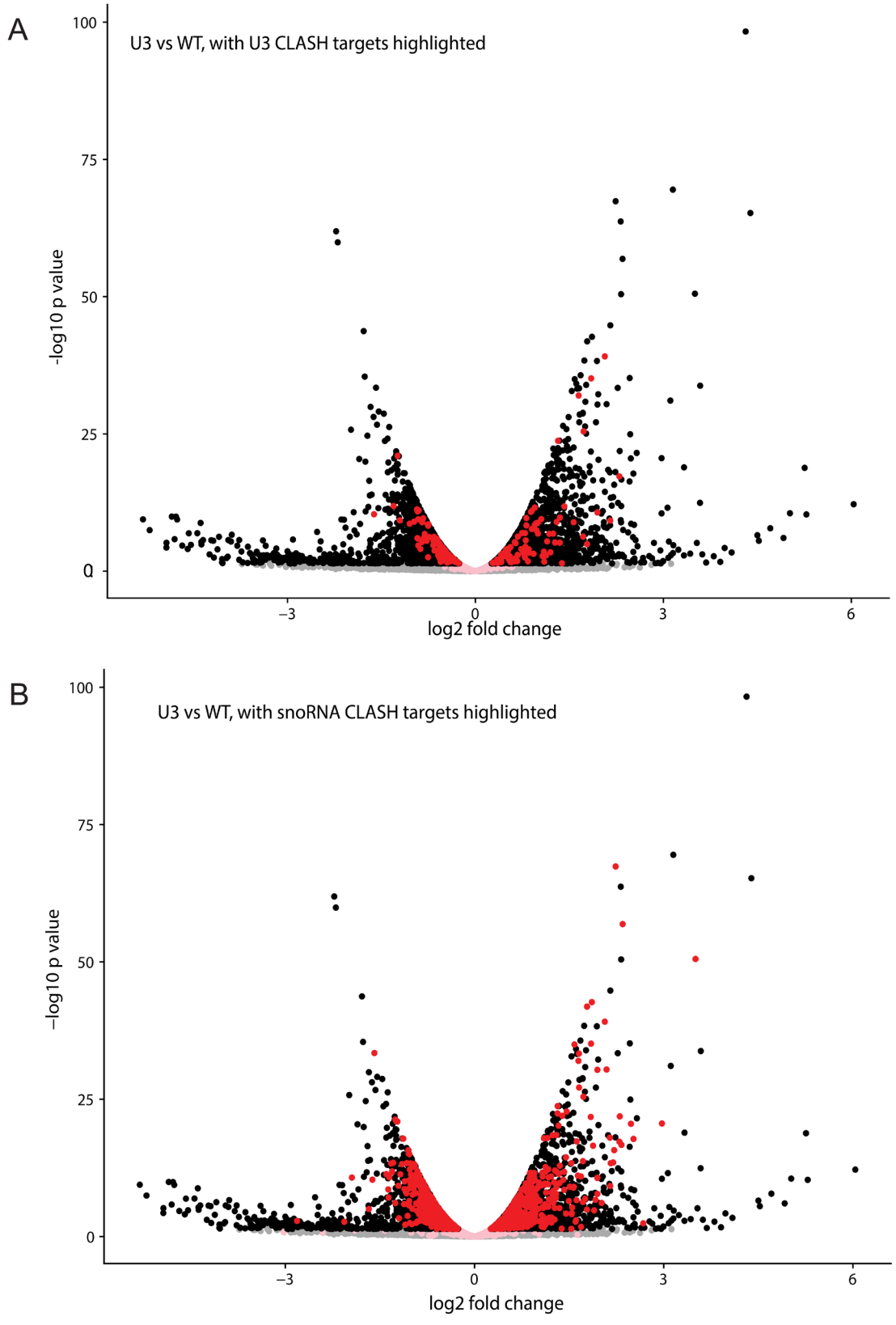

Figure 8. Differential RNA expression in strains expressing mutant U3. Volcano plot showing differential RNA expression in strains expressing mutant U3 compared to the wild type following growth in glucose medium for 36 h. RNA sequencing was performed following Ribominus selection. X axis shows $\log_2$ of normalized RNA fold change with negative values signifying decreased in RNA expression in the mutant. Y axis shows $-\log_{10}$ of the p-value. Significantly differentially expressed genes are either black (non-CLASH targets) or red (CLASH targets). (**A**) U3 targets are highlighted in red; (**B**) All snoRNA targets are highlighted in red.

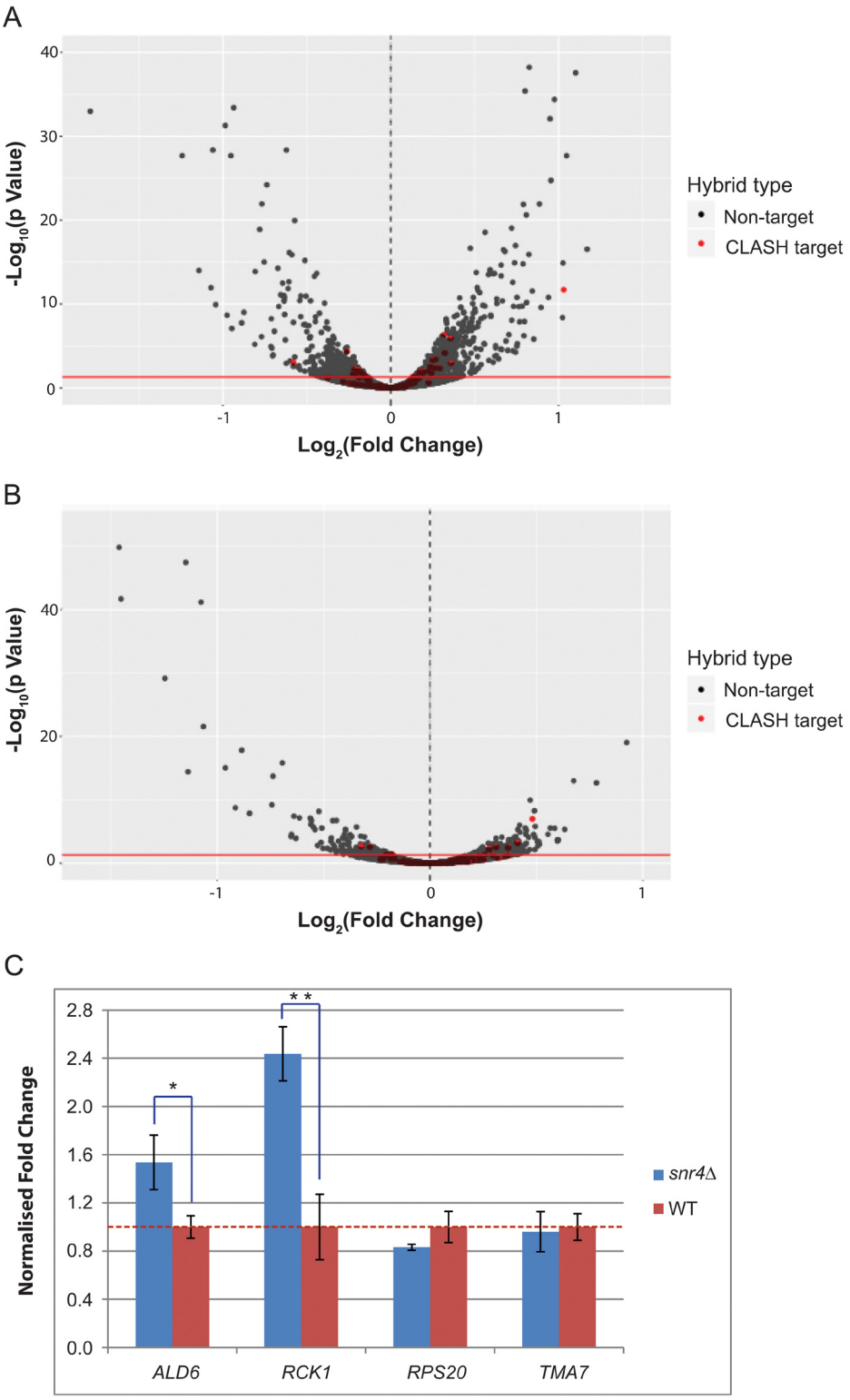

Figure 9. Volcano plot showing differential expression of RNAs during snoRNA deletion, using poly(A)+ selected samples. (**A**) Differential expression of poly(A)-tailed RNAs following growth in standard conditions in *snr4Δ*, compared to WT. The dotted line at 0 signifies normalized WT RNA expression level. Negative values show a decrease in RNA expression, while positive values signify an increase in RNA expression upon snoRNA deletion. Y axis shows –log10 of adjusted p value. Red line indicates p=0.05. Red dots indicate a direct target from CLASH data. (**B**) As in 'A', but harvested transfer for 20 min into the media containing 2% EtOH/glycerol as the carbon source. (**C**) RT-qPCRs showing fold change of CLASH targets following growth in standard conditions. Fold change of snR4 targets in the *snr4Δ* strain compared to WT strain. All samples were normalized to S. pombe *ACT1*, then to *TAF10*, then to WT gene expression level. Red dotted line denotes relative WT expression level. RT was performed using oligo (dT) primers. One asterisk denotes p<0.05, two asterisks denote p<0.01.

snoRNP proteins as bait. The previously described, cognate snoRNA-rRNA pairs were recovered for most sites of yeast rRNA methylation. A further yeast snoRNA-rRNA interaction matched the consensus for methylation guide activity, but did not correspond to a reported site of methylation. In addition, we recovered a large number of snoRNA-rRNA interactions that are not predicted to direct methylation, but which would be expected to block methylation-guide interactions by other snoRNA species. Recent data point to the regulation of rRNA methylation levels in human cells (see for example (Erales *et al.*, 2017); reviewed by (Sloan *et al.*, 2017)) and at least one methylation and a pseudouridine site in the yeast rRNA are substoichiometric (Buchhaupt *et al.*, 2014; Taoka *et al.*, 2016). Competitive interactions between snoRNAs offer a possible mechanism for regulating modification efficiencies.

CLASH analyses with the RNA helicase and surveillance factor Mtr4 revealed a significantly different pattern from the snoRNP proteins. Interactions between snoRNAs and rRNAs identified in association with Mtr4, predominately occurred at methylation sites. However, only a small fraction (~7%) represented cognate methylation guide interactions, compared to the ~60% cognate interactions identified with the snoRNP proteins. It was previously reported that the helicase Prp43 plays a role in unwinding cognate snoRNA-rRNA interactions (Bohnsack *et al.*, 2009). CLASH data are not available for Prp43, but the snoRNAs most frequently bound (snR51, snR72 and snR60) show only limited overlap with the major interactors for Mtr4 (snR128, snR17a, snR55, snR60, snR69). We predict that Mtr4 plays an important surveillance role in dissociating incorrect but stable snoRNA interactions. The basis of the recognition of these interactions remains unclear. However, we note that the yeast snoRNAs are of low abundance relative to the high rate of ribosome synthesis, implying rapid release following RNA modification (Bohnsack *et al.*, 2008). The extended base-paired interactions between snoRNAs and targets are expected to be very stable under physiological conditions, indicating the need for helicase activities. It seems feasible that productive, cognate snoRNA-target interactions are rapidly recognized and dissociated, whereas the non-cognate interactions are of longer duration. This could lead to backup recognition by the nuclear RNA surveillance system, of which Mtr4 is a key component.

A high prevalence of pre-snoRNA binding to other snoRNAs was observed. This could reflect compartmentalization, with enrichment of pre-snoRNAs in a subnuclear, or subnucleolar, region. An obvious possible domain would be the nucleolar body, in which snoRNA cap hypermethylation and snoRNP assembly are reported to occur (Mouaikel *et al.*, 2002; Verheggen *et al.*, 2002). Interactions between different snoRNAs also have an obvious potential to regulate effective snoRNA availability and therefore methylation efficiency.

There are two yeast snoRNAs that have no known participation in ribosome synthesis, snR4 and snR45, and we therefore analyzed these species in more detail. Examining the conservation between distantly related fungi revealed that both *SNR4* and *SNR45* are well-conserved C/D box snoRNAs. However, both showed a pattern of conservation that was different from that of canonical box C/D snoRNAs, particularly in sequences flanking the box motifs, and each contained a similarly positioned region of high conservation that did not correspond to known structural features or the location of a methylation guide sequence. During this work, snR4 and snR45 were shown to guide C5 acetylation by the acetyl-transferase Kre33p of residues C1280 and C1773, respectively, in yeast 18S rRNA (Sharma *et al.*, 2017). Inspection of the snoRNA-rRNA hybrids identified base-pairing between the conserved regions and the sites of rRNA acetylation. More extensive base-pairing between snR4, snR45 and U13, and the 18S rRNA in the vicinity of the acetylation sites have been proposed (Sharma *et al.*, 2017). However, we did not recover hybrids corresponding to these potential interactions

A large number of stable, reproducible snoRNA-mRNA interactions were also identified. It is currently unclear whether any of these mRNAs are actually targets for methylation, or the subcellular location of the interactions. snoRNA-mRNA interactions in the nucleolus are possible, but in metazoans snoRNAs and snRNAs undergo modification in the Cajal bodies. In yeast, snoRNA modification takes place in nucleolar bodies, which appears to be a potential site for snoRNA-mRNA binding. It is also worth noting that, although the nucleolus appears to be a stable structure when visualized in microscopy, or indeed when isolated from the cell, this impression is actually quite misleading. Nucleolar components have long been known to exchange rapidly with free cytoplasmic pools, a phenomenon that now seems likely to be due to the phase-separated nature of the nucleolus. Thus we cannot exclude the possibility that snoRNP-mRNA interactions take place in the nucleoplasm.

We observed that the absence of snR4 or mutation of U3 was associated with altered abundances of relatively small numbers of mRNA species. RNAs that were also identified as CLASH targets were statistically over-represented among mRNAs with altered abundance. Loss of snR4 was preferentially associated with decreased levels of target RNAs, potentially indicating a role in mRNA stabilization. A potential explanation might be that the snoRNP competes with one of more pre-mRNA binding protein(s) that protect the pre-mRNA and/or promote export. However, we cannot exclude the possibility that the snoRNP interacts with the nuclear RNA surveillance machinery to accelerate or retard degradation. In contrast, both increased and decreased levels were observed among U3 target mRNAs. U3 depletion was also associated with altered abundance of other snoRNAs. This could reflect either direct interactions or via the stalled pre-rRNA processing which in turn changed the levels of their target mRNAs too. These observations suggest the evolution of a fast, regulatory mechanism required for stress response during sudden changes in growth conditions.

Data availability

All sequence data from this study have been submitted to the NCBI Gene Expression Omnibus. Sequence data from the CLASH

experiments are available under accession number GSE114680: http://identifiers.org/geo/GSE114680. Sequence data from U3 and snR4 depletion experiments are available under accession number GSE118369: http://identifiers.org/geo/GSE118369

Data generated through the identification of potential novel RNA targets for box C/D snoRNAs in budding yeast are available on figshare: https://doi.org/10.6084/m9.figshare.6984971 (Dudnakova *et al*., 2018).

Grant information

This work was supported by Wellcome Trust Fellowships to D.T. [077248] and R.P. [102311]. T.D and H.D.-D. were supported by BBSRC funding [Bb/L020416/1]. Work in the Wellcome Trust Centre for Cell Biology is supported by Wellcome Trust core funding [092076].

The funders had no role in study design, data collection and analysis, decision to publish, or preparation of the manuscript.

Supplementary material

Supplementary Figure 1. Distribution of protein crosslinking sites by RNA type.
(A) Nop1 CLASH single hits; (B) Nop56 CLASH single hits; (C) Nop58 CLASH single hits.

Click here to access the data

Supplementary Figure 2. Recovered snoRNA-rRNA hybrids overlapping known rRNA methylation sites.
All non-identical snoRNA chimeras mapped to rRNA were tabulated. For each snoRNA, numbers are indicated for all interactions overlapping 2'-O-methylation site. (A) Numbers recovered in the current study. (B) Previously reported numbers of snoRNA-rRNA interactions (Kudla *et al.*, 2011). This dataset contained 25,486 distinct hybrids, of which 3,995 are snoRNA-rRNA hybrids. Within this dataset, we found snoRNA-rRNA hybrids for 37 of the 43 C/D box snoRNAs reported to methylate yeast rRNA in the SnOPY database. For 27 of these snoRNAs, hybrids overlapped the cognate rRNA methylation site.

Click here to access the data

Supplementary Figure 3. RDN37 chimeric hits over SNR4.
(A) Yeast grown in synthetic medium containing 2% glucose. (B) Yeast transferred to synthetic medium containing 2% EtOH/Glycerol for 20 min.

Click here to access the data

Supplementary Figure 4. Wild type and mutant U3 strains.
(A) Wild type U3 (SNR17A/B) interactions over rDNA locus RDN37. (B) RDN37 interactions over SNR17A gene (intron included). (C) Growth rates of strains expressing wild-type U3, the mutant U3, or depleted for U3, following transfer to glucose medium.

Click here to access the data

Supplementary Figure 5.
(A) Growth curve (OD600) of snr4Δ, snr45Δ, HISMX6-PGAL1-SNR45 snr4Δ, HISMX6-PGAL1-SNR4 snr45Δ and wild type in minimal medium containing 2% w/v glucose. A total of three biological replicates were grown, with three technical replicates analyzed for each. A key indicating strains is shown to the right of each panel. (B) snR45-18S rRNA hybrid from yeast CLASH. The acetylated cytosine is indicated in red. Watson-Crick base-pairs, denoted by a blue line; G-U base-pairings are denoted by a dot. Dashed line denotes the boundary between snoRNA and rRNA regions of the hybrid. Hybrid drawn from full chimeric sequence from NOP1 CLASH, and base-pairing predicted using the ViennaRNA package. (C) U13-18S rRNA hybrid from human Fibrillarin CLASH data. (D) Alignment between snR45 and its fungal and human homologues. Conserved C and D boxes are indicated along with the sequence identified in the hybrid with 18S rRNA flanking A1773. Red indicates conservation of ≥90%, blue indicates ≥50% conservation, and black is <50% conserved.

Click here to access the data

Supplementary Figure 6. Interactions between snR4 and 18S rRNA.
(A, B) snR4-18S rRNA hybrids from CLASH. The acetylated cytosine is indicated in the hybrid drawn from full chimeric sequence from Nop1p/Fibrillarin CLASH, and base-pairing predicted using the ViennaRNA package. (C) Alignment between snR4 and fungal homologues. Conserved C and D boxes are indicated along with the sequence identified in the hybrid with 18S rRNA flanking A1280. Red indicates conservation of ≥90%, blue indicates ≥50% conservation, and black is <50% conserved.

Click here to access the data

Supplementary Figure 7. Correlations for all reproducible mRNA hybrids.
(A) Correlation heatmap. (B) Correlation between single hits and chimeric hits. (C) Correlation between hybrid hits and mRNA expression.

Click here to access the data

Supplementary Table 1. Oligonucleotides used in this work.

Click here to access the data

Supplementary Table 2. snoRNA-rRNA interactions at rRNA methylation sites.
Column A: snoRNA - the name of the known snoRNA involved in the interaction. Column B: subunit - rRNA subunit involved in the interaction. Column C: coordinate - the position of the methylated nucleotide in the rRNA subunit. Column D: Overlapping (O/L) (Kudla *et al.*, 2011) - number of hybrids overlapping the methylation site (obtained from data reported by Kudla *et al.*, 2011). Column E: Overlapping (O/L) this study – number of hybrids overlapping the methylation site (obtained from the current study). Column F: Kudla *et al.*, (2011), methylating - number of hybrids overlapping with the methylation site that can support methylation of the rRNA target nucleotide (obtained from Kudla *et al.*, 2011 data). Column G: this study, methylating - number of hybrids overlapping with the methylation site that can support methylation of the rRNA target nucleotide (obtained from the current study). Column H: blocking_current_meth_snoRNAs - number of chimeras formed by the "cognate" snoRNA (known to bind at this site, as in column A) but unable to guide methylation and thus blocking the correct base pairing at the site. Column I: blocking_range_meth_snoRNAs – the name of the snoRNA guiding methylation at the neighboring site and thus blocking the base pairing of the cognate snoRNA at the site. Column J: blocking_range_meth_snoRNAs_No - number of hybrids formed by the neighboring snoRNA and thus blocking the binding of the cognate snoRNA at the site. Column K: blocking_other_meth_snoRNAs – the name of the snoRNA blocking the interaction of the cognate snoRNA but NOT guiding methylation at the neighboring site (possibly binding conventionally elsewhere in the rRNA). Column L: blocking_other_meth_snoRNAs_No – number of hybrids formed at this position by the blocking snoRNA named in Column K.

Click here to access the data

Supplementary Table 3. All snoRNA-mRNA interactions for combined NOP1 datasets
Excel spreadsheet listing all snoRNA-mRNA interactions in the combined NOP1 datasets. The first worksheet lists all of the interactions found, along with the hybrid counts for experiments performed in glucose and ethanol in separate columns. The second and third worksheets show clusters of hybrid hits in the combined glucose and ethanol datasets, created using the combine_hyb_merge script from the hyb package (Travis *et al.*, 2014). The cluster descriptions include the gene based co-ordinates of each fragment (where each gene includes a 20 base pair flank on each end).

Click here to access the data

Supplementary Table 4. All snoRNA-mRNA interactions for combined NOP proteins
Excel spreadsheet listing all snoRNA-mRNA interactions in the combined NOP protein datasets. The first worksheet lists all of the interactions found, along with the hybrid counts, for all hybrids, and reproducible hybrids with a predicted binding energy below -12dG. The second worksheet shows clusters of hybrid hits in the set of reproducible hybrids. The clusters were generated using the same method as in Supplementary Table 3.

Click here to access the data

Supplementary Table 5. snoRNA-mRNA potentially directing RNA methylation.
Column A: methsite_id – position of the potentially methylated nucleotide in the target mRNA. Column B: hybrid_snoRNA – the name of the snoRNA potentially guiding methylation. Column C: hybrid_count – the number of snoRNA-mRNA chimeras supporting potential methylation at the site. Column D: experiment_count – the number of individual experiments from which the hybrids were obtained. Column E: box – the name of the snoRNA box upstream of which the interaction is taking place.

Click here to access the data

References

Anders S, Pyl PT, Huber W: **HTSeq--a Python framework to work with high-throughput sequencing data.** *Bioinformatics.* 2015; **31**(2): 166–169.
PubMed Abstract | Publisher Full Text | Free Full Text

Bolger AM, Lohse M, Usadel B: **Trimmomatic: a flexible trimmer for Illumina sequence data.** *Bioinformatics.* 2014; **30**(15): 2114–2120.
PubMed Abstract | Publisher Full Text | Free Full Text

Bohnsack MT, Kos M, Tollervey D: **Quantitative analysis of snoRNA association with pre-ribosomes and release of snR30 by Rok1 helicase.** *EMBO Rep.* 2008; **9**(12): 1230–1236.
PubMed Abstract | Publisher Full Text | Free Full Text

Bohnsack MT, Martin R, Granneman S, *et al.*: **Prp43 bound at different sites on the pre-rRNA performs distinct functions in ribosome synthesis.** *Mol Cell.* 2009; **36**(4): 583–592.
PubMed Abstract | Publisher Full Text | Free Full Text

Bray NL, Pimentel H, Melsted P, *et al.*: **Near-optimal probabilistic RNA-seq quantification.** *Nat Biotechnol.* 2016; **34**(5): 525–527.
PubMed Abstract | Publisher Full Text

Buchhaupt M, Sharma S, Kellner S, *et al.*: **Partial methylation at Am100 in 18S rRNA of baker's yeast reveals ribosome heterogeneity on the level of eukaryotic rRNA modification.** *PLoS One.* 2014; **9**(2): e89640.
PubMed Abstract | Publisher Full Text | Free Full Text

Corpet F: **Multiple sequence alignment with hierarchical clustering.** *Nucleic*

Acids Res. 1988; **16**(22): 10881–10890.
PubMed Abstract | Publisher Full Text | Free Full Text

Dandekar T, Tollervey D: **Cloning of *Schizosaccharomyces pombe* genes encoding the U1, U2, U3 and U4 snRNAs.** *Gene.* 1989; **81**(2): 227–235.
PubMed Abstract | Publisher Full Text

Delan-Forino C, Schneider C, Tollervey D: **Transcriptome-wide analysis of alternative routes for RNA substrates into the exosome complex.** *PLoS Genet.* 2017; **13**(3): e1006699.
PubMed Abstract | Publisher Full Text | Free Full Text

Dobin A, Davis CA, Schlesinger F, *et al.*: **STAR: ultrafast universal RNA-seq aligner.** *Bioinformatics.* 2013; **29**(1): 15–21.
PubMed Abstract | Publisher Full Text | Free Full Text

Dudnakova T, Dunn-Davies H, Peters R, *et al.*: **Data generated through the identification of potential novel RNA targets for box C/D snoRNAs in budding yeast.** *figshare.* Dataset. 2018.
http://www.doi.org/10.6084/m9.figshare.6984971

Dunn-Davies HR: **hybtools**. 2018.
Reference Source

Erales J, Marchand V, Panthu B, *et al.*: **Evidence for rRNA 2'-O-methylation plasticity: Control of intrinsic translational capabilities of human ribosomes.** *Proc Natl Acad Sci U S A.* 2017; **114**(49): 12934–12939.
PubMed Abstract | Publisher Full Text | Free Full Text

Frazer LN, O'Keefe RT: **A new series of yeast shuttle vectors for the recovery and identification of multiple plasmids from *Saccharomyces cerevisiae*.** *Yeast.* 2007; **24**(9): 777–789.
PubMed Abstract | Publisher Full Text

Gordon A: **Fastx toolkit**. 2010.
Reference Source

Granneman S, Kudla G, Petfalski E, *et al.*: **Identification of protein binding sites on U3 snoRNA and pre-rRNA by UV cross-linking and high-throughput analysis of cDNAs.** *Proc Natl Acad Sci U S A.* 2009; **106**(24): 9613–9818.
PubMed Abstract | Publisher Full Text | Free Full Text

Granneman S, Petfalski E, Tollervey D: **A cluster of ribosome synthesis factors regulate pre-rRNA folding and 5.8S rRNA maturation by the Rat1 exonuclease.** *EMBO J.* 2011; **30**(19): 4006–4019.
PubMed Abstract | Publisher Full Text | Free Full Text

Gumienny R, Jedlinski DJ, Schmidt A, *et al.*: **High-throughput identification of C/D box snoRNA targets with CLIP and RiboMeth-seq.** *Nucleic Acids Res.* 2017; **45**(5): 2341–2353.
PubMed Abstract | Publisher Full Text | Free Full Text

Helwak A, Kudla G, Dudnakova T, *et al.*: **Mapping the human miRNA interactome by CLASH reveals frequent noncanonical binding.** *Cell.* 2013; **153**(3): 654–665.
PubMed Abstract | Publisher Full Text | Free Full Text

Jorjani H, Kehr S, Jedlinski DJ, *et al.*: **An updated human snoRNAome.** *Nucleic Acids Res.* 2016; **44**(11): 5068–5082.
PubMed Abstract | Publisher Full Text | Free Full Text

Kudla G, Granneman S, Hahn D, *et al.*: **Cross-linking, ligation, and sequencing of hybrids reveals RNA-RNA interactions in yeast.** *Proc Natl Acad Sci U S A.* 2011; **108**(24): 10010–10015.
PubMed Abstract | Publisher Full Text | Free Full Text

Lestrade L, Weber MJ: **snoRNA-LBME-db, a comprehensive database of human H/ACA and C/D box snoRNAs.** *Nucleic Acids Res.* 2006; **34**(Database issue): D158–D162.
PubMed Abstract | Publisher Full Text | Free Full Text

Longtine MS, McKenzie A 3rd, Demarini DJ, *et al.*: **Additional modules for versatile and economical PCR-based gene deletion and modification in *Saccharomyces cerevisiae*.** *Yeast.* 1998; **14**(10): 953–961.
PubMed Abstract | Publisher Full Text

Lorenz R, Bernhart SH, Höner zu Siederdissen C, *et al.*: **ViennaRNA Package 2.0.** *Algorithms Mol Biol.* 2011; **6**: 26.
PubMed Abstract | Publisher Full Text | Free Full Text

Love MI, Huber W, Anders S: **Moderated estimation of fold change and dispersion for RNA-seq data with DESeq2.** *Genome Biol.* 2014; **15**(12): 550.
PubMed Abstract | Publisher Full Text | Free Full Text

Lowe TM, Eddy SR: **A computational screen for methylation guide snoRNAs in yeast.** *Science.* 1999; **283**(5405): 1168–1171.
PubMed Abstract | Publisher Full Text

Lu Z, Zhang QC, Lee B, *et al.*: **RNA Duplex Map in Living Cells Reveals Higher-Order Transcriptome Structure.** *Cell.* 2016; **165**(5): 1267–1279.
PubMed Abstract | Publisher Full Text | Free Full Text

Mouaikel J, Verheggen C, Bertrand E, *et al.*: **Hypermethylation of the cap structure of both yeast snRNAs and snoRNAs requires a conserved methyltransferase that is localized to the nucleolus.** *Mol Cell.* 2002; **9**(4): 891–901.
PubMed Abstract | Publisher Full Text

Omer AD, Lowe TM, Russell AG, *et al.*: **Homologs of small nucleolar RNAs in Archaea.** *Science.* 2000; **288**(5465): 517–522.
PubMed Abstract | Publisher Full Text

Pimentel H, Bray NL, Puente S, *et al.*: **Differential analysis of RNA-seq incorporating quantification uncertainty.** *Nat Methods.* 2017; **14**(7): 687–690.
PubMed Abstract | Publisher Full Text

Samarsky DA, Fournier MJ: **Functional mapping of the U3 small nucleolar RNA from the yeast *Saccharomyces cerevisiae*.** *Mol Cell Biol.* 1998; **18**(6): 3431–3444.
PubMed Abstract | Publisher Full Text | Free Full Text

Sharma E, Sterne-Weiler T, O'Hanlon D, *et al.*: **Global Mapping of Human RNA-RNA Interactions.** *Mol Cell.* 2016; **62**(4): 618–626.
PubMed Abstract | Publisher Full Text

Sharma S, Langhendries JL, Watzinger P, *et al.*: **Yeast Kre33 and human NAT10 are conserved 18S rRNA cytosine acetyltransferases that modify tRNAs assisted by the adaptor Tan1/THUMPD1.** *Nucleic Acids Res.* 2015; **43**(4): 2242–2258.
PubMed Abstract | Publisher Full Text | Free Full Text

Sharma S, Yang J, van Nues R, *et al.*: **Specialized box C/D snoRNPs act as antisense guides to target RNA base acetylation.** *PLoS Genet.* 2017; **13**(5): e1006804.
PubMed Abstract | Publisher Full Text | Free Full Text

Sloan KE, Warda AS, Sharma S, *et al.*: **Tuning the ribosome: The influence of rRNA modification on eukaryotic ribosome biogenesis and function.** *RNA Biol.* 2017; **14**(9): 1138–1152.
PubMed Abstract | Publisher Full Text | Free Full Text

Sugimoto Y, Vigilante A, Darbo E, *et al.*: **hiCLIP reveals the *in vivo* atlas of mRNA secondary structures recognized by Staufen 1.** *Nature.* 2015; **519**(7544): 491–494.
PubMed Abstract | Publisher Full Text | Free Full Text

Taoka M, Nobe Y, Yamaki Y, *et al.*: **The complete chemical structure of *Saccharomyces cerevisiae* rRNA: partial pseudouridylation of U2345 in 25S rRNA by snoRNA snR9.** *Nucleic Acids Res.* 2016; **44**(18): 8951–8961.
PubMed Abstract | Publisher Full Text | Free Full Text

Tollervey D, Kiss T: **Function and synthesis of small nucleolar RNAs.** *Curr Opin Cell Biol.* 1997; **9**(3x): 337–342.
PubMed Abstract | Publisher Full Text

Travis AJ, Moody J, Helwak A, *et al.*: **Hyb: a bioinformatics pipeline for the analysis of CLASH (crosslinking, ligation and sequencing of hybrids) data.** *Methods.* 2014; **65**(3): 263–273.
PubMed Abstract | Publisher Full Text | Free Full Text

Tuck AC, Tollervey D: **A transcriptome-wide atlas of RNP composition reveals diverse classes of mRNAs and lncRNAs.** *Cell.* 2013; **154**(5): 996–1009.
PubMed Abstract | Publisher Full Text | Free Full Text

Venema J, Vos HR, Faber AW, *et al.*: **Yeast Rrp9p is an evolutionarily conserved U3 snoRNP protein essential for early pre-rRNA processing cleavages and requires box C for its association.** *RNA.* 2000; **6**(11): 1660–71.
PubMed Abstract | Publisher Full Text | Free Full Text

Verheggen C, Lafontaine DL, Samarsky D, *et al.*: **Mammalian and yeast U3 snoRNPs are matured in specific and related nuclear compartments.** *EMBO J.* 2002; **21**(11): 2736–2745.
PubMed Abstract | Publisher Full Text | Free Full Text

Watkins NJ, Bohnsack MT: **The box C/D and H/ACA snoRNPs: key players in the modification, processing and the dynamic folding of ribosomal RNA.** *Wiley Interdiscip Rev RNA.* 2012; **3**(3): 397–414.
PubMed Abstract | Publisher Full Text

Yang J, Sharma S, Watzinger P, *et al.*: **Mapping of Complete Set of Ribose and Base Modifications of Yeast rRNA by RP-HPLC and Mung Bean Nuclease Assay.** *PLoS One.* 2016; **11**(12): e0168873.
PubMed Abstract | Publisher Full Text | Free Full Text

Yoshihama M, Nakao A, Kenmochi N: **snOPY: a small nucleolar RNA orthological gene database.** *BMC Res Notes.* 2013; **6**: 426.
PubMed Abstract | Publisher Full Text | Free Full Text

Zhang L, Lin J, Ye K: **Structural and functional analysis of the U3 snoRNA binding protein Rrp9.** *RNA.* 2013; **19**(5): 701–711.
PubMed Abstract | Publisher Full Text | Free Full Text

Open Peer Review

Current Peer Review Status: ✔ ✔ ✔ ✔ ✔

Version 2

Reviewer Report 26 November 2018

https://doi.org/10.21956/wellcomeopenres.16240.r34323

✔ **Lars Wieslander**
Department of Molecular Biosciences, The Wenner-Gren Institute, Stockholm University, Stockholm, Sweden

Competing Interests: No competing interests were disclosed.

I have read this submission. I believe that I have an appropriate level of expertise to confirm that it is of an acceptable scientific standard.

Version 1

Reviewer Report 22 October 2018

https://doi.org/10.21956/wellcomeopenres.16053.r33939

✔ **Pascale Romby**
CNRS, Architecture and Reactivity of RNA (ARN), UPR 9002, University of Strasbourg, Strasbourg, France

RNA-RNA pairings are playing numerous roles in living organisms across kingdoms. Their identification, monitoring their dynamics and their functional inputs are still challenging tasks. Recent works enable at the genomic scale the mapping of RNA-RNA interactions using crosslinking followed by ligation of RNA hybrids and high-throughput sequencing. Such a method has been used in this work to map the targets of the box C/D small nucleolar RNAs using key protein partners (Nop1, Nop56 and Nop58) as the baits. This

study identifies large sets of pairings involving most of the known snoRNAs and supports previous findings that the primary function of C/D box snoRNAs is to induce methylation at specific nucleotides of rRNAs. However, this work reveals unexpected findings such as the binding of snoRNAs at rRNA sites, which are not modified, or the binding between two snoRNAs. Interestingly, the CLASH approach was also conducted on the RNA helicase Mtr4 and the data revealed that minority of snoRNA-rRNA interactions predicted to guide methylation was recovered. This allows the authors to propose that Mtr4 is aimed to dissociate inappropriate snoRNA-rRNA interactions. Although the manuscript did not show any mechanistic studies validating the mechanisms of action of snoRNA on mRNAs for instance, the work is certainly of interest and will be useful for the community working on snoRNAs. It opens also new ideas and concepts of RNA regulation.

Minor comments:
1- Most of the snoRNAs were recovered by the CLASH approach except snR53, snR65 and snR78. Is there an explanation? Are these three snoRNAs expressed at low levels or under peculiar conditions of growth?
2- The data obtained on Mtr4 are really of interest. However this is not clear to me whether the other types of interactions (snoRNA-snoRNA, snoRNA-mRNA) were also identified as possible targets for Mrt4. This might also provide some clues whether these potential interactions might be inappropriate or are endowed with regulatory functions.
3- More discussion on the snoRNA-mRNA interactions would be appropriate. Do specific snoRNA target mRNAs that are functionally related? It is claimed that some of the mRNAs might be modified. Do these modifications take place in the coding regions or in the UTRs of the mRNA? The authors have mentioned that most snoRNA-mRNA duplexes are predicted to represent structural interactions. They should clarify what do they mean by structural interactions.
4- The deletion of snR4 or mutation in U3 caused alteration of the steady state yields only of a few number of mRNA targets. Deletion of snR4 decreases the levels of target mRNAs while U3 mutations causes both enhanced and decreased levels of mRNA targets. Is there a possible correlation between the position of the snoRNA binding site on the mRNA and their effect on the mRNA yield?

Is the work clearly and accurately presented and does it cite the current literature?
Yes

Is the study design appropriate and is the work technically sound?
Yes

Are sufficient details of methods and analysis provided to allow replication by others?
Yes

If applicable, is the statistical analysis and its interpretation appropriate?
Yes

Are all the source data underlying the results available to ensure full reproducibility?
Yes

Are the conclusions drawn adequately supported by the results?
Yes

Competing Interests: No competing interests were disclosed.

I have read this submission. I believe that I have an appropriate level of expertise to confirm that it is of an acceptable scientific standard.

Reviewer Report 08 October 2018

https://doi.org/10.21956/wellcomeopenres.16053.r33942

Joshua Black
University of Texas at Austin, Austin, TX, USA
Arlen W. Johnson
Department of Molecular Biosciences, University of Texas at Austin, Austin, TX, USA

In this paper, the authors present a large amount of CLASH data and bioinformatics analysis on RNA hybrids that crosslink to Nop1, Nop56, Nop58 and Mtr4. The sequencing depth allows them to identify numerous unexpected RNA duplexes formed by various snoRNAs. The data could be a resource for others interested in novel functions of snoRNAs but as is, the paper is largely descriptive. Several comments regarding the work:

Major points:

1. There has been some speculation that snoRNA directed modification of mRNAs under stress conditions results from off targeting when ribosome production is reduced. Does the data presented reveal anything to address this idea?

1. Related to Figure 4. Panel A – nucleotides should all be ribonucleotides if this is RNA. The Ts should be Us in the expanded image on the right. Was there any rationale for inserting snR77 sequence into U3? Does the U3mut enter into the SSU Processome? Its phenotype appears to mimic that of cells lacking U3. This leads us to question whether the U3mut enters the SSU Processome. I did not find results to support the statement “We demonstrate that U3 binding in 18S is functionally important.” However, this is well established in previously published work from this lab.

2. Related to Figure 5. The authors propose a model that Mtr4 has a role in unwinding non-cognate snoRNA-rRNA duplexes. This has also been proposed for Prp43. Some comparison with Prp43 would be instructive.

3. The conclusion that Mtr4 is removing snoRNAs comes from comparing the Mtr4 CLASH hybrids are compared to Nop1 hybrids. However, a better comparison would be Nop1 hybrids +/- Mtr4 or Mtr4 hybrids +/-Rrp6 or other exosome mutants. In addition, Nop1 gives 100- to 1000-fold higher reads for hybrids than does Mtr4. What is to be made of the very low recovery of hybrids in the Mtr4 sample?

1. The sections beginning Depletion of U3 and Depletion of snR4 are redundant with earlier sections and should be rearranged to avoid this.

Minor comments:

1. In the last paragraph of page 10, the authors state, “Strains carrying *snr4Δ* or *snr45Δ* showed no detectable growth defect relative to the isogenic wild-type (Supplementary Figure 4D and Dudnakova et al., 2018).” There is no Supplementary Figure 4D.

2. Also, the last line of page 10: “It seemed possible that snR4 and snR45 might have redundant functions, and we therefore generated double mutant strains carrying *HISMX6-PGAL1::SNR45 snr4Δ* and *HISMX6-PGAL1- SNR4* ***snr45***.”

This should read “*snr45*Δ”.

Is the work clearly and accurately presented and does it cite the current literature?
Partly

Is the study design appropriate and is the work technically sound?
Yes

Are sufficient details of methods and analysis provided to allow replication by others?
Yes

If applicable, is the statistical analysis and its interpretation appropriate?
I cannot comment. A qualified statistician is required.

Are all the source data underlying the results available to ensure full reproducibility?
Yes

Are the conclusions drawn adequately supported by the results?
Yes

Competing Interests: No competing interests were disclosed.

We have read this submission. We believe that we have an appropriate level of expertise to confirm that it is of an acceptable scientific standard.

Reviewer Report 03 October 2018

https://doi.org/10.21956/wellcomeopenres.16053.r33938

Carla Columbano Oliveira
Department of Biochemistry, Institute of Chemistry, University of Sao Paulo, São Paulo, Brazil

In this article, the authors show the use of a crosslinking and sequencing of hybrids (CLASH) approach to analyze snoRNA-rRNA interactions and determine the targets of heretofore considered orphan snoRNAs. In addition, the authors identified snoRNAs binding sites to rRNAs that may compete with cognate

snoRNA binding, thereby inhibiting rRNA methylation.

To identify box C/D snoRNP targets, the authors used tagged C/D core proteins Nop1, Nop56 and Nop58 under control of their endogenous promoters. The results show that most of the targets corresponded to rRNA methylation sites, as expected. Interestingly, the same kind of experiments performed with tagged Mtr4 showed non-cognate rRNA regions, raising the hypothesis that this RNA helicase could be responsible for displacing non-cognate snoRNAs.

The snoRNA-snoRNA interactions identified here are suggested to represent regulatory regions in pre-snoRNAs, which could be important for retention, or compartmentalization of snoRNAs.

The authors also report snoRNA-mRNA interactions, including some that might promote methylation of the target mRNAs. These results are very interesting and could assign function to as yet considered orphan snoRNAs.

In summary, this article shows the results of large-scale assessment of box C/D snoRNPs interactions, revealing known and additional targets of these snoRNPs, which can suggest a much broader role for box C/D complexes in posttranscriptional control of gene expression.

Suggestions and some points for discussion:

Introduction, pg. 3:
“Each region is bound by a copy of Nop1, so the regions flanking either box D, box D’ or both can function as methylation guides. The strict requirement for a long region of prefect complementarity that extends to box D/D’ for guide function implies that strong snoRNA base pairing could occur without eliciting target RNA methylation.”
Which region? Sentence should be modified for clarity.
Typo: perfect

Fig. 2A:
In the case of competing snoRNAs of box C/D binding to rRNA, it would be interesting to check whether there are resulting alternative methylation sites on rRNAs.

Fig. 4:
The roles of U3 snoRNP and Rrp9 in pre-rRNA have already been described by the Tollervey group and others. Therefore, the relevance of the results shown in Fig 4 were not entirely clear to me. I suggest clarification of this part.
Interestingly, however, Nop1 seems to bind more efficiently to U3m than to WT U3, although the authors considered it to bind both snoRNAs with equal affinity. The effect is even more evident when considering the fact that Rrp9 does not bind U3 mut.

Page 10, snR4 and snR45:
Was the hypothesis that these two snoRNAs could have redundant functions based only on the observation that they are not essential? This should be better explained.

Pg 17: “We predict that Mtr4 plays an important surveillance role in dissociating incorrect but stable snoRNA interactions.”
The hypothesis of Mtr4 displacing non-cognate snoRNA-rRNA binding is very interesting, but it is not

clear to me how Mtr4 would distinguish between correct and incorrect stable interactions.

Fig. 5D:
Color coding is confusing.

Fig. 6:
Other than the pre-snoRNAs snR17A and 17B that undergo splicing, have the snoRNAs isolated here been shown to be transcribed as longer precursor RNAs that are processed to shorter mature RNAs? From the figure, I gather that some of them are longer at the 5' region, while others are longer at the 3' region.

snoRNA-mRNA interactions: is there any evidence that mRNAs are methylated by Nop1? If mRNAs are methylated by Nop1, this modification should take place in the nucleolus, where Nop1 is localized. Would the authors predict that mRNAs are directed to the nucleolus for methylation?

What would be the mechanism by which snR4 controls levels of mRNAs?

Is the work clearly and accurately presented and does it cite the current literature?
Yes

Is the study design appropriate and is the work technically sound?
Yes

Are sufficient details of methods and analysis provided to allow replication by others?
Yes

If applicable, is the statistical analysis and its interpretation appropriate?
Yes

Are all the source data underlying the results available to ensure full reproducibility?
Yes

Are the conclusions drawn adequately supported by the results?
Yes

Competing Interests: No competing interests were disclosed.

I have read this submission. I believe that I have an appropriate level of expertise to confirm that it is of an acceptable scientific standard.

Reviewer Report 03 October 2018

https://doi.org/10.21956/wellcomeopenres.16053.r33941

Lars Wieslander
Department of Molecular Biosciences, The Wenner-Gren Institute, Stockholm University, Stockholm, Sweden

I think that this article reports sound results. The authors explore a method previously introduced (partly) by the authors to comprehensively map interactions between snoRNAs and various other RNAs, especially rRNA. These data considerably add to our current knowledge about snoRNA function. I have very little to say about the data. Materials and methods are extensive, possibly somewhat difficult to follow in relation to the results. For example, quantitative PCR comes up twice as does RNA library preparation. Perhaps some help to relate to what parts of the results could be given. Also, in some parts the descriptions are detailed (for example polyA selection), while other parts could give some more information (for example, I would have liked to know the hybridization temperature and washing conditions for Northerns). A very small correction: “in functionally” to “is functionally” on page 10, right column, 6 line from end of next to last paragraph.

Is the work clearly and accurately presented and does it cite the current literature?
Yes

Is the study design appropriate and is the work technically sound?
Yes

Are sufficient details of methods and analysis provided to allow replication by others?
Yes

If applicable, is the statistical analysis and its interpretation appropriate?
I cannot comment. A qualified statistician is required.

Are all the source data underlying the results available to ensure full reproducibility?
Yes

Are the conclusions drawn adequately supported by the results?
Yes

Competing Interests: No competing interests were disclosed.

Reviewer Expertise: Gene expression, pre-mRNA processing, ribosome synthesis

I have read this submission. I believe that I have an appropriate level of expertise to confirm that it is of an acceptable scientific standard.

Reviewer Report 01 October 2018

https://doi.org/10.21956/wellcomeopenres.16053.r33940

Bruno Charpentier
CNRS (French National Center for Scientific Research), Molecular Engineering and Articular Physiopathology (IMoPA), University of Lorraine, Nancy, France
Mathieu Rederstorff
CNRS (French National Center for Scientific Research), Molecular Engineering and Articular Physiopathology (IMoPA), University of Lorraine, Nancy, France

The research article by Dudnakova *et al.* from the D. Tollervey lab reports the observation of RNA targets for snoRNAs in yeast, using the CLASH sequencing technique. The issue addressed is of great importance to understand the activity of ribonucleoproteins carrying non coding RNAs that serve as a guide for these activities. The article is well written and scientifically sound.

Most of the reported data are confirmative of previous knowledge in *S. cerevisiae*, bringing only limited novel information, but which however proves the robustness of the approach to isolate snoRNA-RNA targets hybrids. Indeed, among the ≈190000 reproducible hybrids retrieved, a large majority corresponded to snoRNAs interactions with rRNAs, as expected, covering most of the known methylation sites in rRNAs. Very interestingly also, two recently described acetylation sites for the snoRNAs snr4 and 45 were detected by the method.

Nevertheless, what constitutes the most exciting part of the article is that the authors also observed possible novel RNA targets for snoRNAs, as well as putatively novel functions. Some hybrids revealed a possible competitive regulatory role for snoRNAs, when they were bound to non-cognate targets. Additionally, the observation of snoRNA/snoRNA hybrids suggests possible cross-regulation between snoRNAs. Interestingly, several hybrids also corresponded to snoRNA/mRNA pairs.

Finally, when CLASH was performed using the helicase Mtr4 rather than C/D box snoRNA core proteins, the snoRNA-rRNA hybrids retrieved corresponded to fewer bona-fide methylation sites, suggesting a possible role for Mtr4 in dissociating non-cognate snoRNA/rRNA interactions.

A large amount of work was accomplished, but the article is rather descriptive and hypothetical. Very interesting aspects are evocated but on which we can only conjecture, such as regulation functions for snoRNA/snoRNA snoRNA/mRNA hybrids or snoRNA/non cognate rRNA hybrids, or the hybrids obtained with Mtr4. No experimental data are yet provided to confirm these assumptions.

Clarifications and minor points:

- The authors mention that some hybrids correspond to non-cognate snoRNAs bound to rRNA methylation sites, possibly blocking methylation. Could the authors clarify this interesting aspect? How does the snoRNAs bind these non-cognate targets?
- The reasons why the authors inserted the box D flanking region of snR77 in the U3 mutant, nor the consequences of this mutation when yeast cells were grown on Glc medium, are not clear. An equivalent mutant was described by Samarsky & Fournier[1] carrying truncation of the three helices (U3del). What is the advantage of substitution with snR77 sequence rather than helix 3 deletion? What is the mRNA target of snR77? Could the authors comment on Rrp9 binding and U3 function/yeast viability taking into account their data and preceding data on *in vitro* and *in vivo* Rrp9 binding on U3 and U3 mutants[2-4].

- snoRNA-snoRNA hybrids revealed potential interactions between mature snoRNAs and precursor forms of target snoRNAs. Figure 6 shows a preferred location in the 3' sequence of the targeted precursor form. The authors could comment on one exception, snr128, which is produced as a bicistronic precursor with snR190.
- pp3, beginning of the second paragraph: it could be interesting to give for non-specialist readers WEB sites dedicated to snoRNA databases.
- pp10, paragraph 2: the authors mention 12% of snoRNA-snoRNA hybrids and then refer to 0.3%. Can they comment on that or does the 0.3% value rather refers to snRNAs?
- Construction of the U3 mutant with conditional expression is partially described at two places in Results section (in page 10 and page 17). It would be good to correct this redundancy and to provide clarification. For instance, it is not clear for non-specialists why as described in page 10, the mutant strain is inviable in Glc medium: the existence of the second SNR17B gene is not clearly explained.
- pp10, last paragraph, the first sentence refers to Supplementary Figure 4D which apparently does not exist.
- It would be good to make homogeneous the writing of the name of the U3 mutant. i.e. U3mut VS U3 mut VS U3m.
- Figures and supp. Figures are of poor resolution.

Typographic errors:
- pp3, first paragraph, lane 22: prefect should be replaced by perfect.
- pp3, at different places in the Methods section a space must be added between the values and the units.
- pp13, first sentence of the second paragraph was probably truncated (Comparison of SNR4 …).
- pp17, second paragraph on the right: BPS should be replaced by PBS.

References

1. Samarsky DA, Fournier MJ: Functional mapping of the U3 small nucleolar RNA from the yeast Saccharomyces cerevisiae.*Mol Cell Biol*. 1998; **18** (6): 3431-44 PubMed Abstract
2. Rothé B, Manival X, Rolland N, Charron C, Senty-Ségault V, Branlant C, Charpentier B: Implication of the box C/D snoRNP assembly factor Rsa1p in U3 snoRNP assembly.*Nucleic Acids Res*. 2017; **45** (12): 7455-7473 PubMed Abstract | Publisher Full Text
3. Cléry A, Senty-Ségault V, Leclerc F, Raué HA, Branlant C: Analysis of sequence and structural features that identify the B/C motif of U3 small nucleolar RNA as the recognition site for the Snu13p-Rrp9p protein pair.*Mol Cell Biol*. 2007; **27** (4): 1191-206 PubMed Abstract | Publisher Full Text
4. Granneman S, Pruijn GJ, Horstman W, van Venrooij WJ, Luhrmann R, Watkins NJ: The hU3-55K protein requires 15.5K binding to the box B/C motif as well as flanking RNA elements for its association with the U3 small nucleolar RNA in Vitro.*J Biol Chem*. 2002; **277** (50): 48490-500 PubMed Abstract | Publisher Full Text

Is the work clearly and accurately presented and does it cite the current literature?
Yes

Is the study design appropriate and is the work technically sound?
Yes

Are sufficient details of methods and analysis provided to allow replication by others?
Yes

If applicable, is the statistical analysis and its interpretation appropriate?
Yes

Are all the source data underlying the results available to ensure full reproducibility?
Yes

Are the conclusions drawn adequately supported by the results?
Yes

Competing Interests: No competing interests were disclosed.

We have read this submission. We believe that we have an appropriate level of expertise to confirm that it is of an acceptable scientific standard.